

Secret Key Agreement with Large Antenna Arrays under the Pilot Contamination Attack

Sanghun Im, *Student Member, IEEE*, Hyongsuk Jeon, *Member, IEEE*, Jinho Choi, *Senior Member, IEEE*,
and Jeongseok Ha, *Member, IEEE*

Abstract—We present a secret key agreement (SKA) protocol for a multi-user time-division duplex system where a base-station (BS) with a large antenna array (LAA) shares secret keys with users in the presence of non-colluding eavesdroppers. In the system, when the BS transmits random sequences to legitimate users for sharing common randomness, the eavesdroppers can attempt the pilot contamination attack (PCA) in which each of eavesdroppers transmits its target user’s training sequence in hopes of acquiring possible information leak by steering beam towards the eavesdropper. We show that there exists a crucial complementary relation between the received signal strengths at the eavesdropper and its target user. This relation tells us that the eavesdropper inevitably leaves a trace that enables us to devise a way of measuring the amount of information leakage to the eavesdropper even if PCA parameters are unknown. To this end, we derive an estimator for the channel gain from the BS to the eavesdropper and propose a rate-adaptation scheme for adjusting the length of secret key under the PCA. Extensive analysis and evaluations are carried out under various setups, which show that the proposed scheme adequately takes advantage of the LAA to establish the secret keys under the PCA.

Index Terms—Channel estimation, information leakage, large antenna arrays, multi-user, pilot contamination attack, secret key generation, time division duplex.

I. INTRODUCTION

The broadcast nature of wireless medium makes wireless communications especially vulnerable to various security threats such as eavesdropping, impersonating, and message modification. However, by establishing secret keys between legitimate terminals through a secret-key agreement (SKA) protocol, such threats can be efficiently nullified. To this end, information theoretic approaches [1]–[5] for the SKA have been proposed and extensively studied. In [1], Wyner considered a scenario called the wiretap channel in which an eavesdropper listens in on communications between legitimate terminals over a noisier channel than the one between legitimate terminals. In the seminar work, it was shown that a pair of legitimate terminals can share a secret key in total ignorance of the eavesdropper with group codes. Later, Csiszár and Körner [3] generalized the Wyner’s original work in [1]. Motivated by the results, a great deal of research has been conducted on SKA over various types of wiretap channels [6]–[10]. However, such SKA schemes seem impractical as most

of studies on code design for wiretap channels are limited to the cases with asymptotically long block lengths [11]–[13] and the assumption of noisier eavesdropper’s channel may not be guaranteed in many cases. In addition, to determine secrecy rates, eavesdropper’s channel quality and/or statistics must be a priori known.

Meanwhile, it was shown in [4] that a secret key can be shared with public discussion even if an eavesdropper has a better channel provided the legitimate terminals have knowledge of the eavesdropper's channel quality. In addition, a practical sequential SKA protocol was introduced by Maurer. The scheme is designed to sequentially perform the following three phases: the advantage distillation [4], information reconciliation [14], and privacy amplification [15] phases. The first phase, i.e. the advantage distillation, enables the legitimate terminals to share correlated random sequences with a higher correlation than the one an eavesdropper acquires even under the condition that neither of the legitimate terminals has an advantage compared to the eavesdropper. In the information reconciliation phase, the legitimate terminals make their correlated random sequences identical by exchanging information over public channel. Finally, each legitimate terminal independently performs the privacy amplification on the identical random sequence to generate a secret key which the eavesdropper is completely ignorant of. The SKA scheme has been adopted in the quantum key distribution (QKD) protocol [16], [17] in which the quantum entanglement is utilized to detect possible eavesdropping of the randomness sharing between two legitimate terminals. Due to the inherent advantage compared to the eavesdropper, the randomness sharing in the QKD protocol can be performed without the advantage distillation phase. After the randomness sharing, the protocol performs the information reconciliation and the privacy amplification. Meanwhile, in wireless communications, there have been a few notable efforts [18]–[20] to realize the randomness sharing by exploiting wireless channel reciprocity.

Recently, cellular systems with large antenna arrays (LAAs¹) have been extensively studied due to their attractive features [21]–[26]. On one hand, a high spectral efficiency can be achievable since small-scale fading and intra-cell interference can be efficiently mitigated by the LAA [21]–[23]. On the other hand, from a security point of view, the LAA is especially advantageous in the sense that a narrower beam formed by the LAA makes the reception at the passive

S. Im, H. Jeon, and J. Ha are with the Department of Electrical Engineering, Korea Advanced Institute of Science and Technology, Daejeon, Korea (e-mail: sh.im@kaist.ac.kr, h.jeon@kaist.ac.kr, jsha@kaist.edu).

J. Choi is with School of Information and Communications, Gwangju Institute of Science and Technology (GIST), Gwangju, Korea (e-mail: ichoi0114@gist.ac.kr).

¹By the LAA, we mean a BS's antenna array of a number of antenna elements and this number is usually much larger than that of users in the cell under the service of the BS.

eavesdropper significantly weakened. Thus, the secrecy rate of wiretap LAA channels grows with the number of transmit antennas [24]–[28]. Sum secrecy rates in multi-user MIMO system have been studied in [27]. Then, the research is further extended to a multi-cell setup [28]. These studies show that the LAA helps wireless systems to have an advantage over eavesdroppers, which is equivalent to performing the advantage distillation phase [29] in the randomness sharing.

This work considers an SKA protocol for the system with LAA based on the sequential three-phase protocol. In particular, the randomness sharing is carried out in such a way that the base-station (BS) first acquires a collection of channel state information (CSI) between the BS and the multiple users from the receptions of orthogonal training sequences simultaneously sent by the users during a fraction of coherence block. Then, the channel reciprocity [30] enables the BS to make a precoding vector for the subsequent downlink data transmission to each of users equipped with a single receive antenna. The BS transmits different random sequences weighted by precoding vectors to the legitimate users during the remaining fraction of the coherence time. The time-division duplex (TDD) mode significantly reduces the channel estimation overhead [21].

In this work, we assume that uncoded random sequences are transmitted and allows some errors to happen over the transmissions. After the downlink transmissions, the BS and users end up having correlated random sequences that are not necessarily identical due to possible errors in the received random sequences. However, the advantage associated with LAA enables the shared random sequences between the BS and legitimate users to have higher correlations than the ones at the passive eavesdroppers when the number of antennas at the BS is sufficiently large. Thus, by performing the subsequent information reconciliation and privacy amplification phases, the BS and users can have identical secret keys in the end. The key agreement protocol we consider in this work can be understood within the theoretical framework of *sender excited* model [31], [32].

However, recently, a serious security weakness of the SKA protocol was discussed by Zhou *et al* in [33] where it was pointed out that the precoding for legitimate users in the LAA-based TDD system is solely determined by CSI estimates based on the uplink training sequences which are exposed to active attacks. As a potential attack, the authors in [33] studied an active eavesdropping attack called *pilot contamination attack* (PCA) in which an eavesdropper transmits the same pilot sequence as the one from a target user for the purpose of tilting the direction of beam towards the eavesdroppers. In particular, by contaminating the pilot sequence, the eavesdropper deceives the BS to make a precoding vector which steers the beam direction from the target user towards the eavesdropper, and the information sent by the BS leaks to the eavesdropper. Since the PCA was first introduced in [33], countermeasures to protect wireless communications from the PCA have not been well investigated, which motivates our work. There have been efforts to detect the PCA in [26], [34] among which the authors in [26] studied a PCA detector and an estimator of the eavesdropper's channel. While the detector utilizes statistics of the received signals at both BS and the

target user, the estimator is based only on the ones at the BS side. Meanwhile, the work in [34] proposed a PCA detection technique which employs random pilots from a set of phase-shift keying symbols. In [35], an SKA protocol under potential PCA was proposed and evaluated. However, the SKA protocol in [35] is inefficient in the sense that the protocol requires multiple coherence blocks and simply discards suspicious packets.

In this paper, based on the three-phase sequential protocol we propose a modified SKA protocol tailored for nullifying the PCA with assumptions: 1) multiple non-colluding eavesdroppers equipped with a single antenna attempt the PCA to their own targets [36]–[38], 2) the BS and legitimate users do not have any prior knowledge of the eavesdroppers such as the number of eavesdroppers in the network, their locations, and their transmit powers used in the PCA, and 3) other cells fully cooperate in a way not to use the training sequences of the users in the process of SKA. Thus, the pilot contaminations to the users in the SKA process come only from the active eavesdroppers employing the PCA if any. The cooperation with other cells can be justified since the SKA session needs to be rarely performed as compared to data transmission. Thus, the system throughput degradation due to the cooperation could be negligible.

The sequential SKA protocol enables us to establish a secret key between legitimate parties even under the PCA if the SKA scheme has knowledge of how much information the active eavesdroppers have gained about the random sequences transmitted by the BS. However, unfortunately, such knowledge is not available. To overcome the technical challenge, the standard sequential SKA protocol must be modified by introducing a mechanism to estimate the amount of information leakage.

The main idea of the proposed SKA is inspired by the QKD protocol [39]–[41]. The security of QKD is based on the principles of quantum mechanics, the no-cloning theorem [42] for example, implying that eavesdropper cannot overhear qubits transmitted from a transmitter to a receiver without introducing detectable anomalies. In the protocol BB84 [39], the legitimate terminals discuss a certain subset of their measurement results to detect the presence of eavesdropping. When eavesdropping is detected, the random sequence obtained from this session is discarded. We find that the wireless system with LAA has a similar property with which the presence of eavesdropper can be detected. That is, there is a complementary relation between the received signal strengths at the target user and eavesdropper. Once an eavesdropper attempts the PCA on a target user, the received signal strength at the target user becomes weaker than the one expected since the beam formed by the BS for the target user is partially steered towards the eavesdropper. Thus, the stronger the PCA, the wider gap between the signal strength measured at the target user and the one expected. In this paper, based on this relation, we derive an estimator to measure the CSI between the BS and eavesdroppers since the CSI is directly proportional to the amount of the information leakage. Then, the BS and the legitimate users can adjust the lengths of secret keys according to the estimated amount of information leakage contrary to the protocol BB84 [39] where the generated secret keys are

discarded when eavesdropping is suspicious. Performances of the proposed scheme are evaluated by conducting comparisons in numerical and analytic ways in various environments. The main contributions of this paper is summarized as follows:

- 1) We first introduce the proposed SKA protocol to defend wireless systems with LAA against the PCA. The impact of the PCA on the performance of the SKA scheme is analyzed in terms of average signal-to-interference-plus-noise power ratios (SINRs) at the target user and eavesdropper. The analysis results clearly show the complementary relation between the average SINRs at the target user and eavesdropper.
- 2) Based on the complementary relation, we derive an estimator for the purpose of estimating the eavesdroppers' channels, i.e. the ones between the BS and eavesdroppers. It will be shown that the estimation results can be utilized for estimating the amount of information leakage during the randomness sharing.
- 3) We evaluate average secret key lengths when the estimate of information leakage is provided to the sequential SKA protocol which adaptively determines the length of resulting secret key. Performance evaluations show that the secrecy outage probability, i.e. the probability not to achieve perfect secrecy, decreases exponentially fast with the number of antennas. In addition, it will be shown that a stronger PCA ironically results in a better system performance, i.e. a lower secrecy outage probability due to the complementary relation.
- 4) Comprehensive performance evaluations are carried out to see trade-offs between the outage probability and average secret key length with different combinations of system parameters, such as the number of users, the number of antennas at the BS, and the lengths of random sequences. The results of performance evaluations enable the system designer to choose appropriate parameters to meet various system requirements.

The rest of the paper is organized as follows. In Section II, we describe the scenario under investigation which includes the proposed SKA protocol, an adversary model, and channel models. In Section III, the complementary relation of the received signal strengths is analyzed by investigating average SINRs at the legitimate user and eavesdropper. Based on the relation, an estimation scheme for the amount of information leakage to eavesdropper is proposed and analyzed. In Section IV, performance evaluations for the proposed estimation scheme are carried out in terms of a normalized mean-square error. In addition, the secrecy outage probability and the average length of secret key are extensively evaluated with various combinations of design parameters. Finally, we make conclusions in Section V.

Notation: Bold face upper and lower case letters are used to denote matrices and vectors, respectively. Transpose and Hermitian are denoted by $(\cdot)^T$ and $(\cdot)^\dagger$, respectively. We use $[x]^+$ for $\max\{0, x\}$. $\mathbf{0}_M$ and \mathbf{I}_M denote the $M \times 1$ all zero vector and $M \times M$ identity matrix, respectively. We use $\|\cdot\|$ for the Euclidean vector norm. A probability density function (pdf) and a conditional pdf are denoted by $f(\cdot)$ and

$f(\cdot|\cdot)$, respectively. When the pdf and the conditional pdf are parameterized by an unknown parameter θ , they are denoted by $f(\cdot; \theta)$ and $f(\cdot|\cdot; \theta)$, respectively.

II. SECRET KEY AGREEMENT SCHEME

A. System model

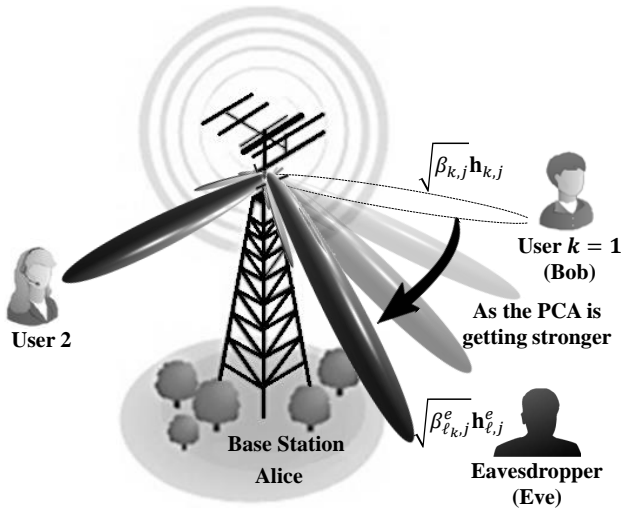
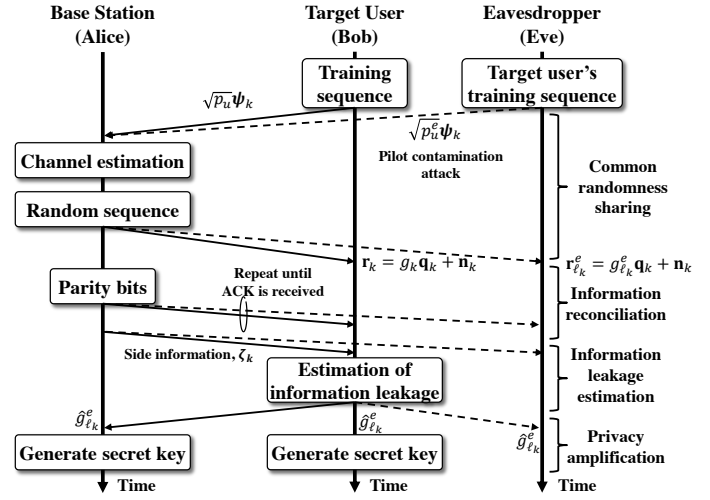
We consider a TDD-based cellular system where a base station in each cell, called *Alice*, aims at establishing different secret keys with K legitimate users in the presence of K_e active eavesdroppers. Alice has an array of a large number of antennas, say M antennas, while each of K users has a single antenna. Fig. 1(a) illustrates an example where the k -th legitimate user is in the SKA session over a wireless channel, and the ℓ_k -th eavesdropper attempts the PCA to the k -th legitimate user over a different wireless channel.

The wireless channels in this work experience both small-scale and large-scale fading. In Fig. 1(a), the channel realization at the j -th coherence block between Alice and the k -th user is given by $\sqrt{\beta_{k,j}}\mathbf{h}_{k,j}$. Here, $\sqrt{\beta_{k,j}}$ accounts for the nonnegative large-scale fading factor determined by path-loss and shadowing, which are slowly varying over time, while $\mathbf{h}_{k,j}$ is an $M \times 1$ vector representing the small-scale fading and varying faster than the large-scale fading factors. We assume that the large-scale fading factors, $\sqrt{\beta_{k,j}}$'s for $1 \leq k \leq K$ are public information a priori known to everyone including eavesdroppers. Meanwhile, it is assumed that the small-scale fading factor, $\mathbf{h}_{k,j}$'s follow $\mathcal{CN}(\mathbf{0}_M, \mathbf{I}_M)$ and are statistically independent and identically distributed (i.i.d.). In addition, we assume block fading channels, i.e. $\mathbf{h}_{k,j}$'s are static over a coherence block and i.i.d. across coherence blocks. The proposed SKA protocol is performed within one coherence block, and thus we will omit the coherence block index j for simplicity throughout this paper. Contrary to the large scaling fading factors, only the statistical properties of the small scale fading factors are known to everyone. Thus, each realization of \mathbf{h}_k is unknown and must be estimated if needed. Similarly, the wireless channels between Alice and the eavesdroppers are modeled as $\sqrt{\beta_\ell^e}\mathbf{h}_\ell^e$, $\ell \in \{1, \dots, K_e\}$, where $\sqrt{\beta_\ell^e}$ and \mathbf{h}_ℓ^e are the large- and small-scale fading factors, respectively. Note that the coherence block index j is omitted as aforementioned. Contrary to the legitimate users' channels, it is assumed that the large scaling fading factors β_ℓ^e is known only to the eavesdroppers, i.e. not available to the legitimate users and Alice.

For the cellular system, we consider the proposed SKA protocol summarized in Fig. 1(b), which consists of common randomness sharing, information reconciliation, information leakage estimation and privacy amplifications. In this section, the building blocks of the proposed scheme in Fig. 1(b) are introduced in detail except for the information leakage estimation which will be discussed in Section III.

B. Common Randomness Sharing (CRS)

1) *Uplink Training:* The CRS is initiated by users who want to establish secret keys. As the first step of the CRS, K users simultaneously transmit orthonormal training sequences at the beginning of a coherence block so that Alice can estimate

(a) Pilot contamination attack for $K = 2$ and $K_e = 1$ 

(b) Secret key generation protocol

Fig. 1. System model

CSI of each user, i.e. \mathbf{h}_k . In particular, the legitimate users transmit $\sqrt{p_u}N_u\psi_k$ to Alice, where p_u is the uplink training power, ψ_k is a $1 \times N_u$ binary orthonormal training sequence, i.e. $\psi_k\psi_k^\dagger = 1$, $\psi_k\psi_\ell^\dagger = 0$ for $k \neq \ell$, and k and ℓ are in $\mathcal{K} = \{1, 2, \dots, K\}$. Here, N_u (i.e., the length of orthonormal training sequences) is usually larger than or equal to K .

Meanwhile, for the PCA, the eavesdroppers inject their target users' training sequences perfectly synchronized with the uplink training sequences originated from the legitimate users. Then, the received signal at Alice becomes

$$\mathbf{Y} = \sum_{k \in \mathcal{K}} \sqrt{p_u \beta_k N_u} \mathbf{h}_k \psi_k + \sum_{\ell \in \mathcal{E}} \sqrt{p_\ell^e \beta_\ell^e N_u} \mathbf{h}_\ell^e \psi_\ell + \mathbf{U}, \quad (1)$$

where $\mathcal{E} = \{1, \dots, K_e\}$ is the index set of eavesdroppers, p_ℓ^e is the PCA power of the ℓ -th eavesdropper, \mathbf{U} is an $M \times N_u$ noise matrix in which each entry is independent zero-mean circularly-symmetric complex Gaussian (CSCG) with unit variance.

Since we assume multiple non-colluding eavesdroppers in a cell, it is conceivable that multiple eavesdroppers may perform the PCA to a target user. This is however of no benefit to the non-colluding eavesdroppers since they are in a competition to pull the user beam towards them, and thereby the amount of information leaked to each eavesdropper decreases. Furthermore, if an eavesdropper performs the PCA on multiple users simultaneously, it will receive a superposition of multiple signals and its eavesdropping performance becomes interference-limited as when a signal to a user is to be detected or decoded, the other signals (to the other users) become interfering signals.

Thus, throughout this paper, we consider the best case scenario for eavesdroppers as follows:

- An eavesdropper does not attempt the PCA targeting more than one user at a time, and
- A user is not targeted by more than one eavesdropper at a time.

The assumptions guarantee that there are at most K eavesdroppers in a cell, i.e. $K_e \leq K$, and each of them has its unique

target. In this work, without loss of generality, we assume that $\mathcal{K} = \mathcal{E}$, i.e. $K_e = K$ and the k -th legitimate user is attacked by the k -th eavesdropper. Hereafter, the k -th user and the k -th eavesdropper are called Bob and Eve for short when there is no risk of confusion.

Since Alice does not know the CSI for the legitimate users, she has to estimate the CSI based on the received signal, \mathbf{Y} . Due to the orthonormality, $\mathbf{y}_k = \mathbf{Y}\psi_k^\dagger$ is a sufficient statistic for estimating the CSI for Bob, i.e. \mathbf{h}_k , which is expressed as

$$\mathbf{y}_k = \sqrt{c_k}(\mathbf{h}_k + w_k \mathbf{h}_k^e) + \mathbf{u}_k, \quad \text{for } k \in \mathcal{K}, \quad (2)$$

where $c_k = p_u \beta_k N_u$, $\mathbf{u}_k = \mathbf{U}\psi_k^\dagger$, and

$$w_k = \sqrt{\frac{p_k^e \beta_k^e}{p_u \beta_k}}, \quad \text{for } k \in \mathcal{K}. \quad (3)$$

In (3), $w_k \in [0, \infty)^2$ represents the effective strength of the PCA to Bob, and the case of $w_k = 0$ implies passive eavesdropping. We employ a minimum mean-square-error (MSE), or MMSE estimator to estimate \mathbf{h}_k [43], [44] which is

$$\hat{\mathbf{h}}_k = \frac{\sqrt{c_k}}{1 + (1 + w_k^2) c_k} \mathbf{y}_k. \quad (4)$$

Note that the estimator in (4) requires the knowledge of w_k that is, however, not available to Alice. Thus, when Alice is not aware of the PCA, she has the estimate, $\hat{\mathbf{h}}_k$ in (4) with $w_k = 0$, which becomes

$$\hat{\mathbf{h}}_k = \mathbf{y}_k \sqrt{c_k} / (1 + c_k).$$

²We exclude $w_k > 1$ since an eavesdropper considered in this paper aims to eavesdrop a secret key between Alice and a target without revealing its presence. Nevertheless, the eavesdropper may increase its uplink training power by $w_k > 1$. In this case, the attack can be detected by the target user immediately [26], and Alice and the target user can avoid such an attack by establishing a new wireless channel to generate a secret key.

2) *Downlink Transmission*: In the downlink transmission, Alice generates K binary random sequences of length N_b , denoted by $\mathbf{b}_k = [b_{k,1}, \dots, b_{k,N_b}]^T$ for $k \in \mathcal{K}$, which are then mapped into a modulated sequence of length N_d , denoted by $\mathbf{q}_k = [q_{k,1}, \dots, q_{k,N_d}]^T$, where $q_{k,j} \in \mathbb{C}$, $1 \leq j \leq N_d$. Alice simultaneously sends \mathbf{q}_k weighted by precoding vectors in the form of $\sqrt{p_d} \sum_{k=1}^K \mathbf{a}_k \mathbf{q}_k^T$ for all $k \in \mathcal{K}$, where p_d is the downlink transmission power, and \mathbf{a}_k is an $M \times 1$ precoding vector for Bob. The average power of \mathbf{q}_k is normalized to be $\frac{1}{N_d} \mathbb{E}[\|\mathbf{q}_k\|^2] = 1$. The precoding vector \mathbf{a}_k is determined as a function of $\hat{\mathbf{h}}_k$, i.e. $\mathbf{a}_k = \varphi(\hat{\mathbf{h}}_k)$ where $\varphi(\cdot)$ is a precoding vector generating function that could be chosen in different ways. In this paper, we consider the matched filter (MF) precoding to gain more insights into the proposed system³:

$$\mathbf{a}_k = \frac{\hat{\mathbf{h}}_k}{\|\hat{\mathbf{h}}_k\|}, \quad \text{for } k \in \mathcal{K}. \quad (5)$$

Meanwhile, at the receiver side, without loss of generality, we assume that the received signal of each user is normalized by $\sqrt{p_d \beta_k M}$ for $k \in \mathcal{K}$. Then, the normalized received signal vector for Bob is given by

$$\mathbf{r}_k = \left(\frac{\mathbf{h}_k^T \mathbf{a}_k}{\sqrt{M}} \right) \mathbf{q}_k + \sum_{\ell \neq k} \left(\frac{\mathbf{h}_k^T \mathbf{a}_\ell}{\sqrt{M}} \right) \mathbf{q}_\ell + \mathbf{z}_k \quad \text{for } k, \ell \in \mathcal{K}, \quad (6)$$

where \mathbf{z}_k is an $N_d \times 1$ zero-mean CSCG noise vector with covariance matrix $(p_d \beta_k M)^{-1} \mathbf{I}_N$. We define an *effective downlink channel gain* (EDCG) from Alice to Bob as $g_k = \frac{1}{\sqrt{M}} \mathbf{h}_k^T \mathbf{a}_k$ which leads to the following simplified expression of \mathbf{r}_k :

$$\mathbf{r}_k = g_k \mathbf{q}_k + \mathbf{n}_k \quad \text{for } k \in \mathcal{K}, \quad (7)$$

where $\mathbf{n}_k = \sum_{\ell \neq k} \left(\frac{\mathbf{h}_k^T \mathbf{a}_\ell}{\sqrt{M}} \right) \mathbf{q}_\ell + \mathbf{z}_k$. In Appendix A, we show that $\mathbf{h}_k^T \mathbf{a}_\ell$ for $k \neq \ell$ follows $\mathcal{CN}(0, 1)$. Thus, the last term, \mathbf{n}_k follows $\mathcal{CN}(\mathbf{0}_{N_d}, \sigma_{n_k}^2 \mathbf{I}_{N_d})$ where

$$\sigma_{n_k}^2 = \frac{1}{M} \left(K - 1 + \frac{1}{p_d \beta_k} \right). \quad (8)$$

Following a similar approach, we have the normalized received signal vector for Eve as

$$\mathbf{r}_k^e = \left(\frac{\mathbf{h}_k^e T \mathbf{a}_k}{\sqrt{M}} \right) \mathbf{q}_k + \sum_{\ell \neq k} \left(\frac{\mathbf{h}_k^e T \mathbf{a}_\ell}{\sqrt{M}} \right) \mathbf{q}_\ell \quad \text{for } k, \ell \in \mathcal{K}. \quad (9)$$

Note that no noise is assumed in the normalized received signal vector for Eve, which leads to an unfavorable scenario to Bob and Alice. Thus, the sum of interference due to the downlink signals to the other users is only the factor to impair recovering \mathbf{q}_k from \mathbf{r}_k^e . In addition, the assumption allows us not to care for the locations of the eavesdroppers. The received signal at Eve, \mathbf{r}_k^e can also be simplified to

$$\mathbf{r}_k^e = g_k^e \mathbf{q}_k + \mathbf{n}_k^e \quad \text{for } k \in \mathcal{E}, \quad (10)$$

³In general, two linear precoding schemes, MF and MMSE precoding methods, are of practical interest [43]. Our main results are also valid with the MMSE precoding, but its complicated expression may make it harder to understand essentials.

where $g_k^e = \frac{1}{\sqrt{M}} \mathbf{h}_k^e T \mathbf{a}_k$ is the EDCG from Alice to Eve, and $\mathbf{n}_k^e = \sum_{\ell \neq k} \left(\frac{\mathbf{h}_k^e T \mathbf{a}_\ell}{\sqrt{M}} \right) \mathbf{q}_\ell$ whose distribution is given by $\mathcal{CN}(\mathbf{0}_{N_d}, \sigma_{n_k^e}^2 \mathbf{I}_{N_d})$ with $\sigma_{n_k^e}^2 = (K - 1)/M$. In Fig. 1(b), the received signals \mathbf{r}_k and \mathbf{r}_k^e at Bob and Eve, respectively, are depicted as the results of the CRS.

C. Information Reconciliation and Privacy Amplification

After the CRS, secret keys are extracted from the shared randomness through the information reconciliation and privacy amplification phases, which requires knowledge of information leakage to eavesdroppers by the PCA. However, we assume that Alice and the K users have no information about eavesdroppers. In this section, we first review the information reconciliation and privacy amplification phases shown in Fig. 1(b) and then discuss how such missing information hinders the phases from generating secret keys.

In the information reconciliation phase, Alice sends parity bits over an *authenticated public channel* to the users who need to correct errors occurred in the CRS. In the CRS, Alice transmits to Bob a sequence \mathbf{q}_k that arrives at Bob and Eve who have received sequences $\mathbf{r}_k = (r_{k,1}, \dots, r_{k,N_d})$ and $\mathbf{r}_k^e = (r_{k,1}^e, \dots, r_{k,N_d}^e)$, respectively. After the randomness sharing, Alice and Bob can have shared information which amounts to $I(\mathbf{Q}_k; \mathbf{R}_k)$ where \mathbf{Q}_k and \mathbf{R}_k are random vectors corresponding to the realizations \mathbf{q}_k and \mathbf{r}_k , respectively. The uncertainty between \mathbf{Q}_k and \mathbf{R}_k must be resolved to make them identical in the information reconciliation phase. According to the Slepian-Wolf theorem [45], the information reconciliation requires at least $\nu_k = H(\mathbf{Q}_k | \mathbf{R}_k) = H(\mathbf{Q}_k) - I(\mathbf{Q}_k; \mathbf{R}_k)$ bit exchanges over the public channel. While either Alice or Bob can generate and transmit the parity bits, this work assumes that Alice sends the parity bits since Alice already has the estimated CSI. Then, Alice and Bob can have an identical sequence, \mathbf{q}_k which turns into the binary sequence, \mathbf{b}_k of length $N_b = H(\mathbf{Q}_k)$. However, the sequence is not secure from eavesdropping due to the information leakage, denoted by \mathbf{E}_k , during the first two phases, i.e. the CRS and information reconciliation phases. Alice and Bob extract a secret key from \mathbf{Q}_k by performing the privacy amplification process which eliminates the amount of eavesdropped information, \mathbf{E}_k , from $H(\mathbf{Q}_k)$. This can be done by using a hash function, $G_k \in \mathcal{G} : \{0, 1\}^{N_b} \rightarrow \{0, 1\}^{s_k}$, randomly chosen from a family of universal hash functions, \mathcal{G} [46] where s_k is the length of secret key, \mathbf{S}_k . If we determine s_k such that

$$s_k = [N_d \{I(Q_k; R_k) - I(Q_k; R_k^e)\} - 2a_k - 2 - b_k]^+, \quad (11)$$

where Q_k and R_k^e are the i.i.d. random variables representing the components in the random vectors, \mathbf{Q}_k and \mathbf{R}_k^e , respectively, it is guaranteed that, for a sufficiently large N_d , the eavesdropper's uncertainty about the secret key, denoted by $H(\mathbf{S}_k | G_k, \mathbf{E}_k)$, is bounded by

$$H(\mathbf{S}_k | G_k, \mathbf{E}_k) \geq s_k - \frac{2^{-b_k}}{\ln 2} \quad \text{with probability } 1 - 2^{-a_k}. \quad (12)$$

By appropriately choosing a_k and b_k , we can obtain a sufficiently long secret key with the eavesdropper's uncertainty that can be arbitrarily close to s_k , which implies perfect secrecy.

However, the standard sequential SKA protocol cannot be directly applied to our scenario due to the assumption, i.e. no prior knowledge about the eavesdroppers. In particular, the problems are as follows:

- 1) Unknown ν_k : The required ν_k for the information reconciliation is derived from $I(Q_k; R_k)$ which is a function of CSI between Alice and Bob. However, once the training sequence sent by Bob is contaminated by the PCA, Alice would have a poor estimate of the CSI, and its corresponding ν_k may not be enough for Bob to decode \mathbf{q}_k .
- 2) Unknown $I(Q_k; R_k^e)$: Due to unknown CSI between Alice and Eve, Alice and Bob cannot measure $I(Q_k; R_k^e)$. Thus, the standard sequential SKA protocol cannot determine the length of secret key in (11) to achieve perfect secrecy.

The first problem of unknown ν_k can be resolved by exchanging additional messages between Alice and Bob. For example, if a rateless Slepian-Wolf code is employed, Alice can repeatedly send additional parity bits to Bob until Bob has a sufficiently large number of parity bits to make \mathbf{r}_k identical to \mathbf{q}_k and sends an acknowledge message to Alice. In this case, although a certain amount of overhead is inevitable, the rateless Slepian-Wolf codes can be a practical solution since they do not require instantaneous CSI between a transmitter and a receiver. Thus, throughout this paper, we assume that Bob can perfectly recover \mathbf{q}_k using a rateless Slepian-Wolf code. The practical design and optimization of rateless Slepian-Wolf codes are presented in [47], [48].

However, unknown $I(Q_k; R_k^e)$ is still problematic. Since the eavesdroppers will not reveal their presence and information about the PCA, a mechanism must be introduced into the proposed scheme to estimate $I(Q_k; R_k^e)$, which is realized in this work by taking advantage of a trace left by the eavesdropper during the PCA. To be precisely, Bob is suspicious of the PCA if its received signal strength unexpectedly drops during the CRS. Then, Bob can estimate $I(Q_k; R_k^e)$ by comparing the received signal strength with its expectation. As depicted in Fig. 1(b), the estimation results, denoted by \hat{g}_k^e , are provided to the privacy amplification, which in the end generates secret keys as the final results of the proposed SKA protocol. The details of the proposed method will be introduced and analyzed in the following sections.

Before finishing this section, a few practical issues should be discussed. In fast fading environments, the proposed SKA protocol may result in a considerable overhead to establish a secret key at a sufficiently long length. In such a case, there might be a trade-off between the data throughput and key renewal rate for a given secret key length. In addition, an unexpected drop of the received signal strength can happen due to user mobility or sudden environment changes, which may introduce a false alarm and thus degrade the performance of the proposed SKA protocol, i.e. the average secret key length.

III. ESTIMATION OF INFORMATION LEAKAGE

In this section, we first investigate an inevitable complementary relation between SINR's at Bob and Eve, i.e. the increase of SINR at one party must result in the decrease of SINR at the other. Based on this complementary relation, we propose an estimator of the EDCG from Alice to Eve (i.e. g_k^e), which allows us to estimate the information leakage to Eve, $I(Q_k; R_k^e)$. The crucial complementary relation also promises a better estimation result for a stronger PCA.

A. The Impact of PCA on Average SINRs

The average SINRs at Bob and Eve, denoted by SINR_k and SINR_k^e , are defined as

$$\text{SINR}_k = \mathbb{E}[(g_k \mathbf{q}_k)^\dagger (g_k \mathbf{q}_k)] / (N_d \mathbb{E}[\mathbf{n}_k^\dagger \mathbf{n}_k]), \text{ and}$$

$$\text{SINR}_k^e = \mathbb{E}[(g_k^e \mathbf{q}_k)^\dagger (g_k^e \mathbf{q}_k)] / (N_d \mathbb{E}[\mathbf{n}_k^{e\dagger} \mathbf{n}_k^e]).$$

Then, the average SINRs are derived in the following result.

Theorem 1: When Bob and Eve receive the signals in (7) and (10), respectively, their SINR's are given by

$$\text{SINR}_k = \frac{Mc_k + w_k^2 c_k + 1}{(1 + (1 + w_k^2) c_k)(K - 1 + \frac{1}{p_d \beta_k})} \text{ and} \quad (13)$$

$$\text{SINR}_k^e = \frac{Mw_k^2 c_k + c_k + 1}{(1 + (1 + w_k^2) c_k)(K - 1)}. \quad (14)$$

Proof: See Appendix B. ■

Remark 1: By letting $w_k \rightarrow 0$, the results in Theorem 1 turn into the ones for passive eavesdropping. Then, we have $\text{SINR}_k = \frac{Mc_k + 1}{(1 + c_k)(K - 1 + \frac{1}{p_d \beta_k})}$ and $\text{SINR}_k^e = (K - 1)^{-1}$, which shows that SINR_k grows with the number of antennas, M . On the other hand, SINR_k^e does not depend on M . Thus, the length of secret key can be increased by employing more antennas at Alice under the passive eavesdropping. While similar results can be found in [24]–[26], the results in the work are different from the previous ones in that the signals for the other $K - 1$ users in our model act as interference and preclude the eavesdropper from taking information.

The ratio of SINR's at Bob and Eve is readily approximated as $\gamma_k = \text{SINR}_k / \text{SINR}_k^e \approx 1/w_k^2$ when $K \gg 1$ and $M \gg 1$. The ratio clearly shows that the SINR at Bob is inversely proportional to the effective strength of the PCA, w_k , which leads to a better SINR at Eve. While the results in Theorem 1 describe the average behavior of SINR, the instantaneous amount of information leakage in each SKA protocol is not provided. In the next subsection, bearing the complementary relation in mind, we will derive an estimator of the EDCG from Alice to Eve, which in turn gives us an instantaneous estimate of the information leakage to eavesdroppers.

B. Estimation of Eavesdropper's Channel

According to (9), the amount of information leaked to Eve, $I(Q_k; R_k^e)$, is readily found by Bob when the EDCG from Alice to Eve, g_k^e is known to Bob. To this end, in this subsection, we derive an estimator for g_k^e . The estimation of g_k^e is carried out by fulfilling a series of estimations: 1) maximum-likelihood estimation (MLE) for w_k 2) MMSE estimation for

g_k , and 3) MMSE estimation for g_k^e , where their estimates are denoted by \hat{w}_k , \hat{g}_k , and \hat{g}_k^e , respectively. The estimation results from the first two steps are used as unknown parameters in the estimations of g_k^e .

The main idea behind the proposed estimator is to exploit the complementary relation between the received signal strengths at Bob and Eve, which results in an unexpected drop of signal strength at the target user when the PCA is attempted to Bob. The difference between the received signal strengths and his expectation will be used to estimate g_k^e . However, the CSI of the channel from Alice to Bob is unknown to Bob and thus he does not know his expected signal strength. To resolve this issue, as shown in Fig. 1(b), Alice sends side information $\zeta_k = \|\mathbf{y}_k\|$ for $k \in \mathcal{K}$, i.e. the strengths of her received signals right after the information reconciliation phase.

1) *Estimation of w_k* : With the side information ζ_k and the normalized received signal vector at Bob in (6), we can derive the MLE, \hat{w}_k , as

$$\hat{w}_k = \arg \max_{w_k} f(\mathbf{r}_k | \mathbf{q}_k, \zeta_k; w_k), \quad (15)$$

where \mathbf{q}_k is given by the information reconciliation using a rateless Slepian-Wolf code. The pdf $f(\mathbf{r}_k | \mathbf{q}_k, \zeta_k; w_k)$ in (15) can be factorized as

$$\begin{aligned} & f(\mathbf{r}_k | \mathbf{q}_k, \zeta_k; w_k) \\ &= \int f(\mathbf{r}_k | \mathbf{q}_k, \zeta_k, g_k; w_k) f(g_k | \mathbf{q}_k, \zeta_k; w_k) dg_k \\ &\stackrel{(a)}{=} \int f(\mathbf{r}_k | \mathbf{q}_k, g_k; w_k) f(g_k | \zeta_k; w_k) dg_k, \end{aligned} \quad (16)$$

where (a) is due to the facts that \mathbf{r}_k is independent of w_k and ζ_k for a given g_k , and g_k is independent of \mathbf{q}_k .

Note that finding \hat{w}_k by substituting (16) into (15) requires an exhaustive search as there is no closed-form solution. It may be impractical to find the estimate by performing numerical integrations, especially when the users suffer from limited computing power and/or power resources. Thus, we approximate the MLE of w_k by taking one of the key features of systems with LAA, i.e. the randomness caused by fading and noise vanishes as the number of antennas increases [22], [23]. The following theorem describes the asymptotic behavior of g_k as $M \rightarrow \infty$.

Theorem 2: Under the PCA with w_k , as M increases, g_k converges to $\mu_{g_k} = \frac{\sqrt{c_k}}{1+(1+w_k^2)c_k} \frac{\zeta_k}{\sqrt{M}}$ in probability for a given ζ_k .

Proof: See Appendix C. ■

Thus, by applying Theorem 2 to (16), we have $f(\mathbf{r}_k | \mathbf{q}_k, g_k; w_k) \rightarrow f(\mathbf{r}_k | \mathbf{q}_k, \mu_{g_k}; w_k)$ in probability for a large M . This result allows us to have a simpler MLE of w_k . That is, the value of w_k for which the derivative of $f(\mathbf{r}_k | \mathbf{q}_k, \mu_{g_k}; w_k)$ with respect to w_k is equal to zero corresponds to \hat{w}_k . After some manipulations, we obtain a closed form expression for \hat{w}_k as

$$\hat{w}_k = \sqrt{\left[\frac{\zeta_k}{\frac{\mathbf{r}_k^\dagger \mathbf{q}_k}{\mathbf{q}_k^\dagger \mathbf{q}_k} \sqrt{c_k M}} - \left(1 + \frac{1}{c_k}\right) \right]^+}. \quad (17)$$

2) *Estimation of g_k* : The MMSE estimator for g_k , i.e. $\hat{g}_k = \mathbb{E}[g_k | \mathbf{r}_k, \mathbf{q}_k, \zeta_k; w_k]$ can be derived as

$$\hat{g}_k = \frac{\mathbf{r}_k^\dagger \mathbf{q}_k + \sigma_{n_k}^2 \mu_{g_k} / \sigma_{g_k}^2}{\mathbf{q}_k^\dagger \mathbf{q}_k + \sigma_{n_k}^2 / \sigma_{g_k}^2}. \quad (18)$$

The details of the derivation are given in Appendix E.

3) *Estimation of g_k^e* : The MMSE estimator for g_k^e is obtained by taking the conditional expectation of g_k^e given the known parameters, \mathbf{r}_k , \mathbf{q}_k , and ζ_k [43]. That is, \hat{g}_k^e is given by

$$\hat{g}_k^e = \mathbb{E}[g_k^e | \mathbf{r}_k, \mathbf{q}_k, \zeta_k; w_k], \quad (19)$$

which is derived in the following theorem.

Theorem 3: For given \mathbf{r}_k , \mathbf{q}_k , and ζ_k , the MMSE estimator for g_k^e is given by

$$\hat{g}_k^e = \frac{w_k c_k}{1 + w_k^2 c_k} \left(\frac{\zeta_k}{\sqrt{c_k M}} - \hat{g}_k \right), \quad (20)$$

where \hat{g}_k is the MMSE estimate of g_k in (18).

Proof: From (19), we can find \hat{g}_k^e by conducting a serious of decomposition as follows:

$$\begin{aligned} \hat{g}_k^e &= \int g_k^e f(g_k^e | \mathbf{r}_k, \mathbf{q}_k, \zeta_k; w_k) dg_k^e \\ &= \int g_k^e \int f(g_k^e, g_k | \mathbf{r}_k, \mathbf{q}_k, \zeta_k; w_k) dg_k dg_k^e \\ &= \int g_k^e \int f(g_k^e | g_k, \mathbf{r}_k, \mathbf{q}_k, \zeta_k; w_k) \\ &\quad f(g_k | \mathbf{r}_k, \mathbf{q}_k, \zeta_k; w_k) dg_k dg_k^e \\ &\stackrel{(a)}{=} \int g_k^e \int f(g_k^e | g_k, \zeta_k; w_k) f(g_k | \mathbf{r}_k, \mathbf{q}_k, \zeta_k; w_k) dg_k dg_k^e \\ &\stackrel{(b)}{=} \int \left[\int g_k^e f(g_k^e | g_k, \zeta_k; w_k) dg_k^e \right] f(g_k | \mathbf{r}_k, \mathbf{q}_k, \zeta_k; w_k) dg_k \\ &\stackrel{(c)}{=} \frac{w_k c_k}{1 + w_k^2 c_k} \left(\frac{\zeta_k}{\sqrt{c_k M}} - \mathbb{E}[g_k | \mathbf{r}_k, \mathbf{q}_k, \zeta_k; w_k] \right), \end{aligned} \quad (21)$$

where (a) is from the fact that g_k^e is independent of \mathbf{r}_k and \mathbf{q}_k for given g_k and ζ_k , (b) is from the Fubini's theorem that allows us to change the order of integration, (c) is from the fact that $\int g_k^e f(g_k^e | g_k, \zeta_k; w_k) dg_k^e = \mu_c$ derived in Appendix D. ■

Remark 2: The expression for \hat{g}_k^e in (20) shows that the estimator exploits the complementary relation as expected. That is, Bob first tries to estimate g_k , and then g_k^e by comparing the estimate of g_k with its expected value, $\frac{\zeta_k}{\sqrt{c_k M}}$. Thus, for a given ζ_k , the smaller \hat{g}_k Bob has, the larger \hat{g}_k^e the estimator produces. In the end, the PCA is detected with the higher probability. It should be noted that while we do not discuss in this work, a detector can be derived with the result in (20) with which the shared random sequence can be discarded when eavesdropping is detected as the BB84 protocol does. In the evaluations of the \hat{g}_k^e , the unknown parameter w_k will be replaced with the estimated one, \hat{w}_k in (17).

In Section IV, the performances of the proposed estimator in (20) will be evaluated in terms of the MSE [43] which is derived in this subsection. Let us first rewrite the estimate of g_k as $\hat{g}_k = g_k - e_{k,1}$, where $e_{k,1}$ is the MMSE estimation

error of \hat{g}_k . Then, the MMSE estimator for g_k^e in (20) can be rewritten as

$$\begin{aligned}\hat{g}_k^e &= \frac{w_k c_k}{1 + w_k^2 c_k} \left(\frac{\zeta_k}{\sqrt{c_k M}} - g_k + e_{k,1} \right) \\ &\stackrel{(a)}{=} \mathbb{E}[g_k^e | \zeta_k, g_k] + \frac{w_k c_k}{1 + w_k^2 c_k} e_{k,1} \\ &= g_k^e - e_{k,2} + \frac{w_k c_k}{1 + w_k^2 c_k} e_{k,1} = g_k^e - e_{k,2} + e'_{k,1}, \quad (22)\end{aligned}$$

where (a) is due to the fact that the conditional mean value of g_k^e for given g_k and ζ_k is $\frac{w_k c_k}{1 + w_k^2 c_k} (\frac{\zeta_k}{\sqrt{c_k M}} - g_k)$ as shown in Appendix D, and $e_{k,2}$ is defined as the MMSE estimation error of g_k^e when g_k is perfectly known to Bob. Thus, the MSE of \hat{g}_k^e becomes

$$\begin{aligned}\mathbb{E}[|\hat{g}_k^e - g_k^e|^2; w_k] &= \mathbb{E}[|e_{k,2}|^2] + \mathbb{E}[|e'_{k,1}|^2] - 2\mathbb{E}[\Re\{e_{k,2}e'_{k,1}\}] \\ &\stackrel{(a)}{=} \mathbb{E}[|e_{k,2}|^2] + \left(\frac{w_k c_k}{1 + w_k^2 c_k} \right)^2 \mathbb{E}[|e_{k,1}|^2],\end{aligned}$$

where (a) is from the facts that $e_{k,2}$ is independent of $e_{k,1}$, and $\mathbb{E}[e_{k,i}] = 0$ for $i = 1, 2$ since the MMSE estimation error is Gaussian with zero mean [43], [44]. Note that $\mathbb{E}[|e_{k,2}|^2]$ and $\mathbb{E}[|e_{k,1}|^2]$ correspond to the conditional variances of g_k^e and g_k with respect to the pdfs $f(g_k^e | \zeta_k, g_k; w_k)$ and $f(g_k | \mathbf{r}_k, \mathbf{q}_k, \zeta_k; w_k)$, respectively, which are derived in Appendices D and E, respectively. Then, the MSE of \hat{g}_k^e is finally given by

$$\begin{aligned}\mathbb{E}[|\hat{g}_k^e - g_k^e|^2; w_k] &= \frac{1}{(1 + w_k^2 c_k)M} + \left(\frac{w_k c_k}{1 + w_k^2 c_k} \right)^2 \frac{\sigma_{g_k}^2 \sigma_{n_k}^2}{\sigma_{g_k}^2 \mathbf{q}_k^\dagger \mathbf{q}_k + \sigma_{n_k}^2} \\ &= \frac{1}{M} \left\{ \frac{1}{1 + w_k^2 c_k} + \frac{\left(\frac{w_k c_k}{1 + w_k^2 c_k} \right)^2}{\frac{\mathbf{q}_k^\dagger \mathbf{q}_k}{(K - 1 + \frac{1}{p_d \beta_k})} + \frac{1 + (1 + w_k^2) c_k}{1 + w_k^2 c_k}} \right\}, \quad (23)\end{aligned}$$

where $\sigma_{n_k}^2$ is taken from (8). The MSE in (23) looks inversely proportional to the number of antennas, M .

Remark 3: Before closing this sub-section, it should be noted that Alice can also transmit downlink pilot signals which may help Bob to estimate the EDCGs, g_k , and g_k^e . Such a two-way training strategy [49], [50] is especially helpful under fast fading environments where the length of random sequence \mathbf{q}_k is limited due to the short coherence time interval. Since the proposed scheme estimates the EDCGs based on the random sequence \mathbf{q}_k , the limited length of random sequence results in poor estimates of g_k and g_k^e . In such a case, it may be beneficial to allocate a portion of the downlink transmission to the downlink pilot signals, which significantly improves the estimates. While the two-way training strategy reduces the length of random sequence, the better estimates of EDCGs may offset the decrease of the length of the random sequence. Thus, by carefully allocating the downlink transmission to the pilot signals and random sequence, a longer secret key may be achievable. As another practical issue, we may need to consider that while this work assumes the perfect channel reciprocity, the uplink and downlink channels may change

during the key sharing process, which increases the channel estimate error. The analysis with the channel variation can be conducted by modifying the derivations for the estimation errors derived in this section.

C. Secret Key Generation

We can now estimate $I(Q_k; R_k^e)$ in (11) by replacing the true value of g_k^e with its estimate, \hat{g}_k^e derived in the previous subsection. Let us denote the estimate of $I(Q_k; R_k^e)$ based on \hat{g}_k^e by $I(Q_k; \hat{R}_k^e)$ with which the length of secret key is now adaptively determined as

$$\hat{s}_k = [N_d \{I(Q_k; R_k) - I(Q_k; \hat{R}_k^e)\} - 2a_k - 2 - b_k]^+ \quad (24)$$

$$\begin{aligned}&= [N_d \{H(Q_k | \hat{R}_k^e) - H(Q_k | R_k)\} - 2a_k - 2 - b_k]^+ \\ &\geq [N_d \{H(Q_k | \hat{R}_k^e) - \nu_k\} - 2a_k - 2 - b_k]^+, \quad (25)\end{aligned}$$

where $\hat{R}_k^e = \hat{g}_k^e Q_k + N_k$ is the output from an AWGN channel with gain \hat{g}_k^e and Gaussian noise N_k , and $\nu_k \geq H(Q_k | R_k)$ is the number of parity bits exchanged in the information reconciliation phase. Later in the performance evaluations, we assume that ν_k equals $H(Q_k | R_k)$, and the equality holds in (25). However, the estimation error in \hat{g}_k^e may result in an underestimate of $I(Q_k; R_k^e)$. According to (12), a secrecy outage occurs when the true value of g_k^e is greater than its estimate, \hat{g}_k^e . In this case, Alice and Bob fail to make the generated secret key completely secure from the eavesdropping. To analyze how often the proposed SKA protocol causes the outage event, we evaluate the secrecy outage probability, i.e. $\Pr(|\hat{g}_k^e| < |g_k^e|)$.

We introduce to the SKA protocol a design parameter called a secrecy margin, $\delta \in [0, \infty)$ to compensate for the estimation error in \hat{g}_k^e and define an outage event as

$$\mathcal{S} = \{|g_k^e|^2 | (1 + \delta)^2 |\hat{g}_k^e|^2 < |g_k^e|^2\}. \quad (26)$$

Then, for given w_k and δ , the secrecy outage probability is expressed as

$$\begin{aligned}P_{\text{out}}(\mathbf{r}_k, \mathbf{q}_k, \zeta_k; w_k, \delta) &= \int_{|g_k^e|^2 \in \mathcal{S}} f(|g_k^e|^2 | \mathbf{r}_k, \mathbf{q}_k, \zeta_k; w_k) d|g_k^e|^2. \quad (27)\end{aligned}$$

Meanwhile, the secrecy margin turns \hat{R}_k^e into $\hat{R}_k^e = (1 + \delta) \hat{g}_k^e Q_k + N_k$, which decreases the secret key length, \hat{s}_k in (24) at the expense of the outage probability.

Since the pdf $f(g_k^e | \mathbf{r}_k, \mathbf{q}_k, \zeta_k; w_k)$ follows $\mathcal{CN}(\mu_{\hat{g}_k^e}, \sigma_{\hat{g}_k^e}^2)$ as shown in Appendix D, the conditional pdf $f(|g_k^e|^2 | \mathbf{r}_k, \mathbf{q}_k, \zeta_k; w_k)$ in (27) follows a Rice distribution. Thus, we can simply express $P_{\text{out}}(\mathbf{r}_k, \mathbf{q}_k, \zeta_k; w_k, \delta)$ in (27) as

$$\begin{aligned}P_{\text{out}}(\mathbf{r}_k, \mathbf{q}_k, \zeta_k; w_k, \delta) &= Q_1 \left(\sqrt{\frac{2|\mu_{\hat{g}_k^e}|^2}{\sigma_{\hat{g}_k^e}^2}}, \sqrt{\frac{2|(1 + \delta)\hat{g}_k^e|^2}{\sigma_{\hat{g}_k^e}^2}} \right), \quad (28)\end{aligned}$$

where $Q_1(a, b) = \int_b^\infty x \exp\left(-\frac{x^2 + a^2}{2}\right) I_0(ax) dx$ is the first order generalized Marcum Q -function, and $I_0(\cdot)$ is the zeroth order modified Bessel function. By averaging the secrecy outage probability in (28) with respect to the joint pdf

$f(\mathbf{r}_k, \mathbf{q}_k, \zeta_k; w_k)$, the average secrecy outage probability is given by

$$\bar{P}_{\text{out}}(w_k, \delta) = \mathbb{E}[P_{\text{out}}(\mathbf{r}_k, \mathbf{q}_k, \zeta_k; w_k, \delta)]. \quad (29)$$

To get more insightful results, we introduce to (28) an upper bound

$$Q_1(a, b) \leq \exp \left[-\frac{(b-a)^2}{2} \right], \quad (30)$$

for $a \leq b$ [51], [52]. Then, the average secrecy outage probability is also bounded as

$$\bar{P}_{\text{out}}(w_k, \delta) \leq \mathbb{E} \left[\exp \left\{ -\frac{(|(1+\delta)\hat{g}_k^e| - |\mu_{\hat{g}_k^e}|)^2}{\sigma_{\hat{g}_k^e}^2} \right\} \right]. \quad (31)$$

Now, it is much easier to investigate into asymptotic behaviors of the average secrecy outage probability with the upper bound in (31). That is, as M grows, the upper bounds in (31) turns into

$$\lim_{M \rightarrow \infty} \bar{P}_{\text{out}}(w_k, \delta) \leq \exp \left[-\frac{(1+w_k^2 c_k) M \delta^2}{1 + \frac{w_k^2 c_k^2 (K-1 + \frac{1}{p_d \beta_k})}{\mathbf{q}_k^\dagger \mathbf{q}_k (1+w_k^2 c_k) + (K-1 + \frac{1}{p_d \beta_k}) \{1+(1+w_k^2) c_k\}}} \right]. \quad (32)$$

since $\hat{g}_k^e \rightarrow \mu_{\hat{g}_k^e}$ in probability.

It can be noticed that the bound in (32) decreases exponentially fast with M , which is possible due to the fact that Bob can accurately adjust the length of extracting secret key as \hat{g}_k^e gets close to g_k^e with the growing number antennas. That is, even if the beam is tilted toward Eve under the PCA, the LAA is still helpful for Bob not only to eliminate the noise/fading effects from the received signal but also to estimate the amount of information leakage. In Section IV, we will analyze the average secrecy outage probability with various combinations of w_k and δ .

IV. PERFORMANCE EVALUATIONS

In this section, we present performances of the proposed SKA protocol in both numerical and analytic ways⁴. Throughout the performance evaluations, we consider the following system setup: the ratios of uplink and downlink transmit powers (p_u and p_d , respectively) to the unit noise variance are set to 10 dB and 20 dB, respectively. This asymmetric power allocation is due to the practical consideration that the power at the user side may be limited. For the downlink transmission, we consider binary random sequences, i.e. $\mathbf{q}_k \in \{-1, 1\}^{N_d}$ for $k \in \mathcal{K}$. While binary sequences are considered in this work, the results can be readily extended to sequences with larger alphabet symbols since all the derivations are in general forms. The large scale fading factors, i.e. β_k and β_ℓ^e , are set to one for all $k, \ell \in \mathcal{K}$. Finally, the number of symbols in the uplink training sequences is assumed to be $N_u = 100$. For the given setup, we will evaluate performances of the proposed

SKA protocol with various combinations of design parameters, M , K , N_d , and δ and show how the parameters affect the performances.

A. Estimation of g_k^e

We first evaluate performances of the estimator \hat{g}_k^e in (20) in terms of the normalized MSE (NMSE) defined as

$$\text{NMSE} = \frac{\mathbb{E}[|g_k^e - \hat{g}_k^e|^2]}{\mathbb{E}[|g_k^e|^2]}. \quad (33)$$

As a reference, we consider the case that g_k is perfectly known to Bob. Then, the NMSE becomes

$$\text{NMSE}_{\text{ideal}} = \frac{1}{\mathbb{E}[|g_k^e|^2]} \frac{1}{(1 + w_k^2 c_k) M}, \quad (34)$$

since the perfect knowledge of g_k makes $e_{k,1}$ in (22) zero. Thus, the ideal NMSE in (34) is a lower bound on the NMSE of \hat{g}_k^e which is taken as a yardstick in the performance evaluations. The NMSE evaluations are carried out with the analytic expression of the MSE in (23) and the estimate of w_k in (17). To confirm the results, we also find an empirical expectation for the NMSE by conducting the estimations of g_k^e and w_k 10^5 times at each point in Figs. 2(a) and 2(b). The evaluations from the two different approaches are completely overlapped each other, which confirms the derivations in Section III.

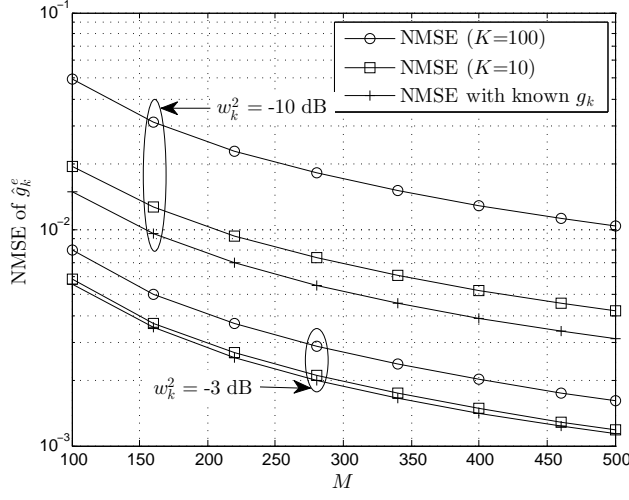
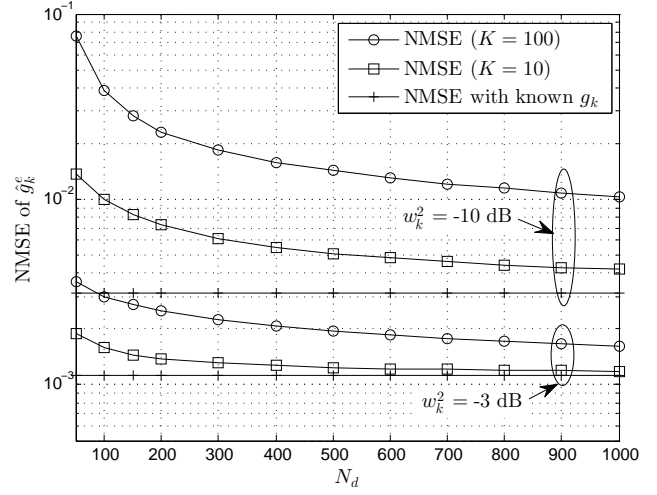
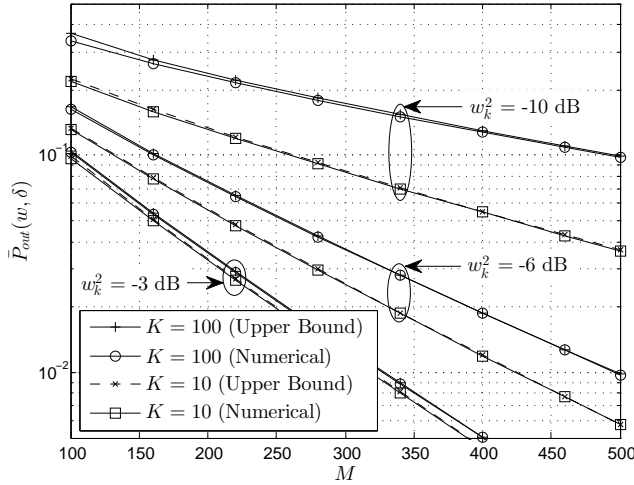
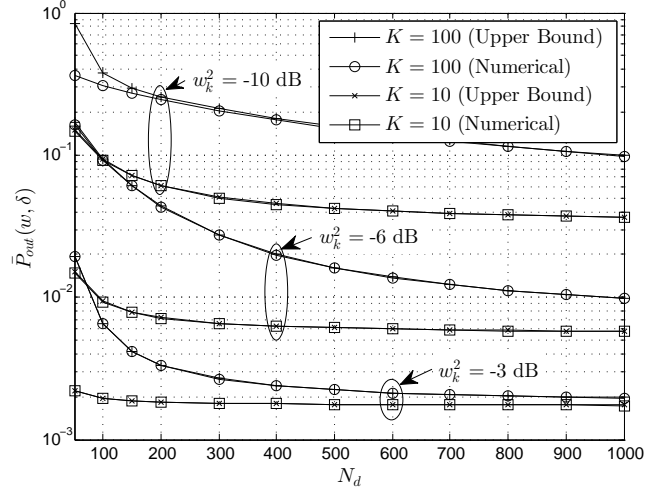
The evaluations of NMSE versus M at different combinations of K and w_k are depicted in Fig. 2(a) where the NMSE decreases as either of M and w_k increases as predicted by the closed-form expression for the MSE in (23). The results in Fig 2(a) imply that for a fixed number of antennas, M , Bob achieves a better estimation of Eve's channel g_k^e when Eve attempts a stronger attack, i.e. a larger PCA power w_k^2 in hopes of eavesdropping more information about the communication between legitimate parties. On the other hand, the increase of the number of users, K , induces more interference to Bob and thus degrades the NMSE. In Fig. 2(b), the NMSE evaluations are performed with respect to N_d at $M = 500$, which shows the same trends as the ones in Fig. 2(a). It is also noticed that the lower bound on NMSE looks independent of N_d , i.e. the length of \mathbf{q}_k since N_d affects only the results of \hat{g}_k as shown in (18), and the lower bound already assumes the true value of g_k . The results in Fig. 2(b) show that the performances of \hat{g}_k^e eventually approaches the lower bounds as N_d increases since the more samples provide the better degree of accuracy in the estimation of g_k [43], [44].

B. Average Secrecy Outage Probability

In this subsection, we present average secrecy outage probability of the proposed SKA protocol. As a performance benchmark, we also plot the upper bound on $\bar{P}_{\text{out}}(w_k, \delta)$ by introducing another upper bound on the Marcum Q -function: (28):

$$\begin{aligned} Q_1(a, b) &\leq \frac{I_0(ab)}{\exp(ab)} \left\{ \exp \left[-\frac{(b-a)^2}{2} \right] + a \sqrt{\frac{\pi}{2}} \text{erfc} \left(\frac{b-a}{\sqrt{2}} \right) \right\}, \end{aligned} \quad (35)$$

⁴Although we also perform Monte Carlo simulations, we do not present the results in this paper as we confirm that our simulation results are exactly the same to the numerical evaluations.

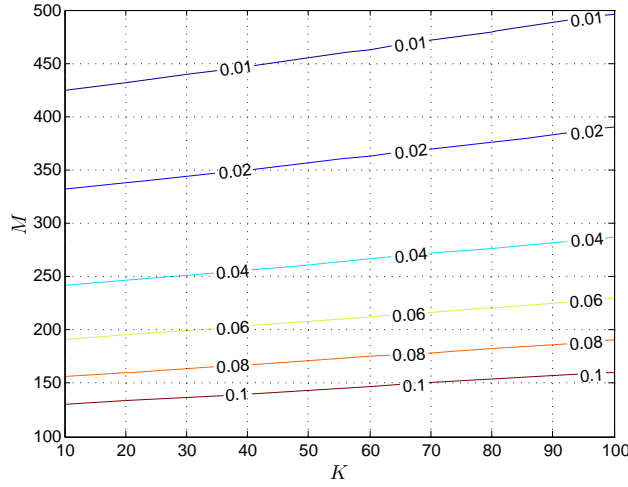
(a) NMSE of \hat{g}_k^e versus M when $N_d = 1,000$.(b) NMSE of \hat{g}_k^e versus N_d when $M = 500$.Fig. 2. NMSE of \hat{g}_k^e with different values of M , K , and N_d .(a) $\bar{P}_{\text{out}}(w_k, \delta)$ versus M when $N_d = 1,000$.(b) $\bar{P}_{\text{out}}(w_k, \delta)$ versus N_d when $M = 500$.Fig. 3. Average secrecy outage probability, $\bar{P}_{\text{out}}(w_k, \delta)$, with different parameters for a fixed $\delta = 0.1$.

where $\text{erfc}(x) = \frac{1}{\pi} \int_x^\infty \exp(-t^2) dt$. Note that although the bound in (35) is less insightful than that in (30), it provides a tighter upper bound than that in (30) [51], [52].

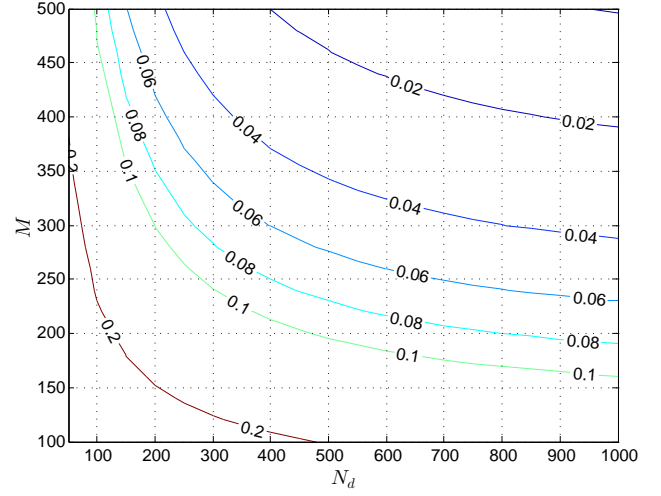
Fig. 3 depicts the average secrecy outage probability, $\bar{P}_{\text{out}}(w_k, \delta)$, with respect to M and N_d for different values of w_k and K when $\delta = 0.1$. The results in Fig. 3(a) show that $\bar{P}_{\text{out}}(w_k, \delta)$ decreases exponentially fast with M as expected from (32). It is also observed that a lower $\bar{P}_{\text{out}}(w_k, \delta)$ is achievable as w_k increases, i.e. a stronger PCA, which is due to the fact that a larger w_k allows the proposed estimator \hat{g}_k^e to have a smaller MSE as derived in (23), and thereby we can reduce the occurrence of secrecy outage events. The secrecy outage probability also decreases as N_d increases as shown in Fig. 3(b), which is due to a better estimate of g_k as observed in Fig. 2(b). For a large N_d , $\bar{P}_{\text{out}}(w_k, \delta)$ eventually converges to a certain value which corresponds to the average outage probability when the true value of g_k is revealed to the

estimator of g_k^e .

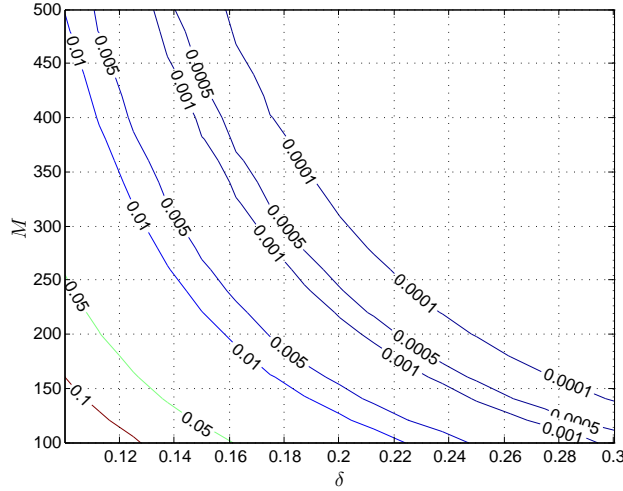
We now see trade-off relations among different parameters, M , K , N_d , and δ , in the average secrecy outage probability by investigating the contour plots of $\bar{P}_{\text{out}}(w_k, \delta)$ in Fig. 4 where w_k^2 is set to -6dB . The results provide a useful reference that enables system designers to select appropriate combinations of system parameters to meet various system requirements. The results in Fig. 4(a) show that the number of antennas M must be almost linearly increased to compensate for the growing number of users K to achieve a target average secrecy outage probability. The tradeoff between M and K is due to the results in (32) where the exponent is inversely proportional to M/K for a large N_d . The average secrecy outage probability is also analyzed with respect to M and N_d in Fig. 4(b) where it is observed that the performance loss caused by employing a smaller size of the LAA can be compensated for by increasing N_d to some extent and vice versa. However, as noticed in Fig.



(a) Contour plot of $\bar{P}_{\text{out}}(w_k, \delta)$ versus M and K when $N_d = 1,000$ and $\delta = 0.1$.



(b) Contour plot of $\bar{P}_{\text{out}}(w_k, \delta)$ versus M and N_d when $K = 100$ and $\delta = 0.1$.



(c) Contour plot of $\bar{P}_{\text{out}}(w_k, \delta)$ versus M and δ when $K = 100$ and $N_d = 1,000$.

Fig. 4. Contour plot of $\bar{P}_{\text{out}}(w_k, \delta)$ when $w_k^2 = -6$ dB

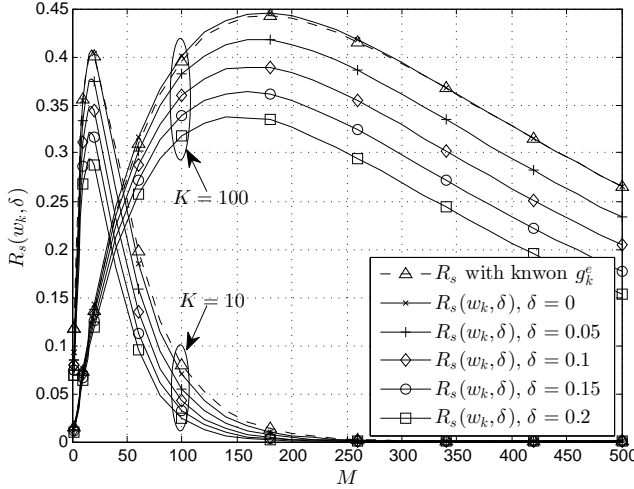
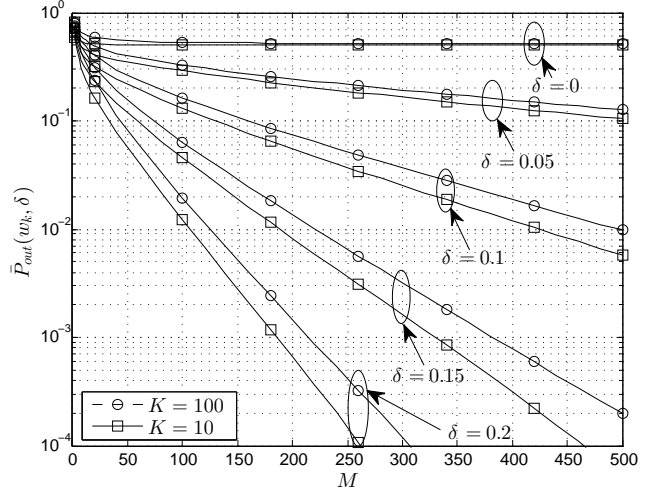
4(b) the impact of N_d on $\bar{P}_{\text{out}}(w_k, \delta)$ is saturated fast with growing N_d . Thus, increasing M is a more effective way to reduce $\bar{P}_{\text{out}}(w_k, \delta)$ when N_d is already large enough. Finally, we see the variations of average secrecy outage probability with respect to the secrecy margin, δ in Fig. 4(c) where it is observed that a small change of δ can exert a large influence on $\bar{P}_{\text{out}}(w_k, \delta)$ since the average outage probability is decreases exponentially fast with respect to the square of the secrecy margin as shown in (32). However, it should be noted that the smaller outage probability is achieved at the expense of the secret key length. We will discuss this issue in detail in the next subsection.

C. Average Length of Extracting Secret Key

In this subsection, we evaluate the average length of secret key in (24) with respect to different values of M and δ when $N_d = 1,000$ and $w_k^2 = -6$ dB. Note that a_k and b_k in (24) become negligible for a sufficiently large N_d [53]. Hence, for

simplicity, we only evaluate $R_s(w_k, \delta) = \mathbb{E}\{[I(Q_k; R_k) - I(Q_k; \hat{R}_k^e)]^+\}$, where the expectation is taken over the joint pdf of $f(\mathbf{r}_k, \mathbf{q}_k, \zeta_k; w_k)$. We also evaluate the average secret key length when the eavesdropper's channel, g_k^e is perfectly known to Bob, $R_s(w_k) = \mathbb{E}\{[I(Q_k; R_k) - I(Q_k; R_k^e)]^+\}$ as a performance benchmark, which elucidates the performance loss due to the error in the estimation of g_k^e .

The average secret key lengths $R_s(w_k, \delta)$ and average secrecy outage probabilities $\bar{P}_{\text{out}}(w, \delta)$ are evaluated in Figs. 5(a) and 5(b), respectively, with respect to M for different values of K and δ . It is noticed that there exists a fundamental trade-off between $R_s(w_k, \delta)$ and $\bar{P}_{\text{out}}(w_k, \delta)$. That is, if we increase δ to achieve a lower $\bar{P}_{\text{out}}(w, \delta)$, we have accordingly a smaller $R_s(w_k, \delta)$. We can also observe that $R_s(w_k, \delta)$ with $\delta = 0$ achieves almost the same performance of $R_s(w_k)$ in Fig. 5(a). This result implies that the proposed estimator \hat{g}_k^e produces an estimate very close to its true value, g_k^e . However, in Fig. 5(b), the corresponding $\bar{P}_{\text{out}}(w_k, \delta)$ approaches almost

(a) $R_s(w_k, \delta)$ versus M .(b) $\bar{P}_{\text{out}}(w_k, \delta)$ versus M with different δ .Fig. 5. $R_s(w_k, \delta)$ and $\bar{P}_{\text{out}}(w_k, \delta)$ with respect to M for $N_d = 1,000$ and $w_k^2 = -6$ dB.

0.5. Note that the estimation result from the MMSE estimator for g_k^e follows a Gaussian distribution [43], [44], and thus $|\hat{g}_k^e|$ follows a Rician distribution. While the Rician distribution is not symmetric with respect to its true value g_k^e , it becomes symmetric as M increases. Thus, for all sufficiently large M , $P_{\text{out}} = \Pr(|\hat{g}_k^e| < |g_k^e|) = \Pr(|\hat{g}_k^e| \geq |g_k^e|) = 0.5$. However, for some small M values, the asymmetry of the Rician distribution makes P_{out} larger than 0.5 as shown in Fig. 5(b). However, the results in (31) tell that $\bar{P}_{\text{out}}(w, \delta)$ decreases exponentially fast with increasing δ , and thus a small sacrifice of $R_s(w_k, \delta)$ is well paid off by a significant improvement of $\bar{P}_{\text{out}}(w, \delta)$.

In Fig. 5(a), it is also noticed that $R_s(w_k, \delta)$ has a peak after which $R_s(w_k, \delta)$ decreases with growing M . This happens due to the fact that both $I(Q_k; R_k)$ and $I(Q_k; R_k^e)$ can not exceed 1 bit per channel-use (bpcu) and are proportional to the size of the LAA as expected from (13). Thus, as M grows, the $R_s(w_k, \delta)$ has a maximum value and later becomes diminished as both $I(Q_k; R_k)$ and $I(Q_k; R_k^e)$ approach 1 bpcu.

V. CONCLUSIONS

We studied an SKA protocol with LAA for a multi-user TDD system in the presence of multiple eavesdroppers attempting the PCA. By exploiting the complementary relation between the received signal strengths at the eavesdropper and its target user, an estimator was derived to measure the EDCG from the BS to the eavesdropper. From an estimated EDCG, the amount of information leakage was quantified, which was used to adaptively adjust the length of extract secret key. Extensive performance evaluations have been carried out in both numerical and analytic ways. We showed that even in the case that the eavesdropper can manipulate the LAA by the PCA, we can still take advantage of the LAA in the estimator and extract a certain length of secret keys with an arbitrary low secrecy outage probability. As future research directions, we will study a coordinated protocol to detect the PCA in a multi-cell scenario, where the reuse of the same training

sequence across cells can be mis-identified as the PCA. In addition, the research will further proceed to the cases when the channels between legitimate parties and eavesdropper are correlated, multiple antennas are employed in eavesdroppers, and the channel reciprocity does not hold due to the channel variations over time for practical considerations.

APPENDIX A

Consider two $M \times 1$ independent random vectors $\mathbf{x} = [x_1, \dots, x_M]^T$ and $\mathbf{y} = [y_1, \dots, y_M]^T$ that are zero-mean CSCG with covariance matrices $\sigma_x^2 \mathbf{I}_M$ and $\sigma_y^2 \mathbf{I}_M$, respectively. Then, the m -th component of \mathbf{y} can be rewritten by $y_m = r_m e^{j\phi_m}$ for $m = 1, \dots, M$ where $r_m \in [0, \infty)$ and $\phi_m \in [-\pi, \pi)$ follow Rayleigh and uniform distributions, respectively. Then, it can be shown

$$t = \mathbf{x}^\dagger \frac{\mathbf{y}}{\|\mathbf{y}\|} = \tilde{x}_1 \tilde{r}_1 + \dots + \tilde{x}_M \tilde{r}_M,$$

where $\tilde{x}_m = x_m e^{j\phi_m}$ and $\tilde{r}_m = \frac{r_m}{\sqrt{r_1^2 + \dots + r_M^2}}$. Note that \tilde{x}_m has the same distribution as x_m due to the circularly-symmetric property. The pdf of t is given by

$$\begin{aligned} f(t) &= \int f(t|\tilde{\mathbf{r}}) f(\tilde{\mathbf{r}}) d\tilde{\mathbf{r}} \\ &\stackrel{(a)}{=} \int \frac{1}{\pi \sigma_x^2 \sum_{m=1}^M \tilde{r}_m^2} \exp\left(-\frac{t^2}{\sigma_x^2 \sum_{m=1}^M \tilde{r}_m^2}\right) f(\tilde{\mathbf{r}}) d\tilde{\mathbf{r}} \\ &\stackrel{(b)}{=} \frac{1}{\pi \sigma_x^2} \exp\left(-\frac{t^2}{\sigma_x^2}\right), \end{aligned}$$

where (a) is due to the fact that t can be seen as the summation of independent complex Gaussian random variables $\{\tilde{x}_m\}$ for given $\tilde{\mathbf{r}} = [\tilde{r}_1, \dots, \tilde{r}_M]^T$, and (b) is due to the fact that $\sum_{m=1}^M \tilde{r}_m^2 = 1$.

APPENDIX B

Since we normalize the average power of \mathbf{q}_k to one, we have $\text{SINR}_k = \frac{\mathbb{E}[|g_k|^2]}{\sigma_{n_k}^2}$ that is determined by the distribution of g_k .

Based on the orthogonality principle of the MMSE estimation [43], [44], we can rewrite g_k as follows:

$$g_k = \frac{\mathbf{h}_k^\dagger \mathbf{a}_k}{\sqrt{M}} \stackrel{(a)}{=} \frac{(\hat{\mathbf{h}}_k + \mathbf{e}_k)^\dagger \hat{\mathbf{h}}_k}{\sqrt{M} \|\hat{\mathbf{h}}_k\|}, \quad (36)$$

where (a) is from $\mathbf{a}_k = \frac{\mathbf{y}_k}{\zeta_k} = \frac{\hat{\mathbf{h}}_k}{\|\hat{\mathbf{h}}_k\|}$, and \mathbf{e}_k is the estimation error of the MMSE estimation. Note that we have $\hat{\mathbf{h}}_k \sim \mathcal{CN}(\mathbf{0}_M, \frac{c_k}{1+(1+w_k^2)c_k} \mathbf{I}_M)$ and $\mathbf{e}_k \sim \mathcal{CN}(\mathbf{0}_M, \frac{1+w_k^2 c_k}{1+(1+w_k^2)c_k} \mathbf{I}_M)$ from the MMSE property [43], [44]. Then, g_k in (36) can be rewritten by

$$g_k = \frac{1}{\sqrt{M}} \left(\|\hat{\mathbf{h}}_k\| + \mathbf{e}_k^\dagger \frac{\hat{\mathbf{h}}_k}{\|\hat{\mathbf{h}}_k\|} \right) \stackrel{(a)}{=} \frac{1}{\sqrt{M}} (\|\hat{\mathbf{h}}_k\| + e_k),$$

where (a) is from Appendix A, and $e_k \sim \mathcal{CN}(0, \frac{1+w_k^2 c_k}{1+(1+w_k^2)c_k})$. We notice that due to the orthogonality principle of the MMSE estimation, we have $\mathbb{E}[\|\hat{\mathbf{h}}_k\| e_k] = 0$. Thus, we have $\mathbb{E}[|g_k|^2] = \frac{1}{M} \mathbb{E}[\|\hat{\mathbf{h}}_k\| + e_k]^2] = \frac{1}{M} \mathbb{E}[\|\hat{\mathbf{h}}_k\|^2] + \frac{1}{M} \mathbb{E}[e_k^2]$. Since both $\hat{\mathbf{h}}_k$ and e_k follow the complex Gaussian distribution, we have $\mathbb{E}[\|\hat{\mathbf{h}}_k\|^2] = \frac{c_k}{2\{1+(1+w_k^2)c_k\}} \mathbb{E}[\mathcal{X}_{2M}^2]$ and $\mathbb{E}[e_k^2] = \frac{1+w_k^2 c_k}{2\{1+(1+w_k^2)c_k\}} \mathbb{E}[\mathcal{X}_2^2]$, where \mathcal{X}_m^2 is a chi-square random variable with m degrees of freedom whose first order moment is $\mathbb{E}[\mathcal{X}_m^2] = m$. Thus, we have $\mathbb{E}[|g_k|^2] = \frac{c_k}{1+(1+w_k^2)c_k} + \frac{1+w_k^2 c_k}{M\{1+(1+w_k^2)c_k\}} = \frac{M c_k + w_k^2 c_k + 1}{M\{1+(1+w_k^2)c_k\}}$. Then, from (8), we finally have

$$\text{SINR}_k = \frac{M c_k + w_k^2 c_k + 1}{(1 + (1 + w_k^2) c_k) (K - 1 + \frac{1}{p_d \beta_k})}.$$

We omit the derivation of SINR_k^e since we can derive SINR_k^e in the same manner.

APPENDIX C

Let us first find the asymptotic behavior of $f(g_k|\zeta_k; w)$. In Appendix D, we have $f(g_k|\zeta_k; w) \sim \mathcal{CN}(\mu_{g_k}, \sigma_{g_k}^2)$. It is obvious that $\lim_{M \rightarrow \infty} \sigma_{g_k}^2 = 0$, while the limiting value of μ_{g_k} is given by

$$\begin{aligned} \lim_{M \rightarrow \infty} \mu_{g_k} &= \lim_{M \rightarrow \infty} \frac{\zeta_k}{\sqrt{M}} \left\{ \frac{\sqrt{c_k}}{1 + (1 + w_k^2) c_k} \right\} \\ &= \lim_{M \rightarrow \infty} \frac{1}{\sqrt{M}} \sqrt{\sum_{m=1}^M |y_{km}|^2} \left\{ \frac{\sqrt{c_k}}{1 + (1 + w_k^2) c_k} \right\} \\ &\stackrel{(a)}{=} \sqrt{\frac{c_k}{1 + (1 + w_k^2) c_k}}, \end{aligned} \quad (37)$$

where y_{km} is the m -th component of \mathbf{y}_k , and (a) is from the law of large numbers that, as M goes to infinity, the sample variance of random variable converges to its true variance. Therefore, for a given ζ_k , $g_k \rightarrow \mu_{g_k}$ in probability as $M \rightarrow \infty$. Then, the asymptotic behavior of $f(g_k; w_k)$ for a large M is

given by

$$\begin{aligned} &\lim_{M \rightarrow \infty} f(g_k; w_k) \\ &= \lim_{M \rightarrow \infty} \int f(g_k|\zeta_k; w_k) f(\zeta_k; w_k) d\zeta_k \\ &\stackrel{(a)}{=} \int \lim_{M \rightarrow \infty} f(g_k|\zeta_k; w_k) f(\zeta_k; w_k) d\zeta_k \\ &\stackrel{(b)}{=} \sqrt{\frac{c_k}{1 + (1 + w_k^2) c_k}} \text{ in probability,} \end{aligned}$$

where (a) is due to the Lebesgue dominated convergence theorem, and (b) is from (37).

APPENDIX D

In this Appendix, we derive various pdfs used in this paper⁵.

A. pdfs of $f(g_k|\zeta_k; w_k)$ and $f(g_k^e|\zeta_k; w_k)$

We first derive the pdf of $f(g_k|\zeta_k; w_k)$. To obtain $f(g_k|\zeta_k; w_k)$, we first derive $f(\mathbf{h}_k|\mathbf{y}_k; w_k)$ using the Baye's theorem, which is given by

$$f(\mathbf{h}_k|\mathbf{y}_k; w_k) = \frac{f(\mathbf{y}_k|\mathbf{h}_k; w_k) f(\mathbf{h}_k)}{f(\mathbf{y}_k; w_k)}, \quad (38)$$

where, from (2), we have $f(\mathbf{y}_k|\mathbf{h}_k; w_k) \sim \mathcal{CN}(\sqrt{c_k} \mathbf{h}_k, (1 + w_k^2 c_k) \mathbf{I}_M)$, $f(\mathbf{h}_k) \sim \mathcal{CN}(\mathbf{0}_M, \mathbf{I}_M)$, and $f(\mathbf{y}_k; w_k) \sim \mathcal{CN}(\mathbf{0}_M, (1 + c_k + w_k^2 c_k) \mathbf{I}_M)$. After some manipulations, we can derive the conditional pdf of $f(\mathbf{h}_k|\mathbf{y}_k; w_k)$ from (38) as follows:

$$f(\mathbf{h}_k|\mathbf{y}_k; w_k) \sim \mathcal{CN}\left(\frac{\sqrt{c_k}}{1 + c_k + w_k^2 c_k} \mathbf{y}_k, \frac{1 + w_k^2 c_k}{1 + c_k + w_k^2 c_k} \mathbf{I}_M\right).$$

Note that $g_k = \mathbf{h}_k^T \mathbf{a}_k / \sqrt{M}$ is the sum of scaled Gaussian random variables for a given \mathbf{y}_k since \mathbf{a}_k becomes constant for a given \mathbf{y}_k . Then, we have $f(g_k|\mathbf{y}_k; w_k) \sim \mathcal{CN}(\mu_{g_k}, \sigma_{g_k}^2)$, where

$$\mu_{g_k} = \frac{\sqrt{c_k}}{1 + c_k + w_k^2 c_k} \frac{\|\mathbf{y}_k\|}{\sqrt{M}} \text{ and } \sigma_{g_k}^2 = \frac{1 + w_k^2 c_k}{(1 + c_k + w_k^2 c_k) M}.$$

Finally, $f(g_k|\|\mathbf{y}_k\|; w_k)$ is derived from $f(g_k|\mathbf{y}_k; w_k)$ as follows:

$$\begin{aligned} f(g_k|\mathbf{y}_k; w_k) &= f(g_k|\mathbf{y}_k, \|\mathbf{y}_k\|; w_k) \\ &\stackrel{(a)}{=} f(g_k|\|\mathbf{y}_k\|; w_k), \end{aligned}$$

where (a) is due to the fact that μ_{g_k} and $\sigma_{g_k}^2$ are independent of \mathbf{y}_k for a given $\|\mathbf{y}_k\|$. In the same manner, we have $f(g_k^e|\zeta_k; w_k) \sim \mathcal{CN}(\mu_{g_k^e}, \sigma_{g_k^e}^2)$, where $\mu_{g_k^e} = \frac{w_k \sqrt{c_k}}{(1 + c_k + w_k^2 c_k) M} \frac{\zeta_k}{\sqrt{M}}$ and $\sigma_{g_k^e}^2 = \frac{1 + c_k}{(1 + c_k + w_k^2 c_k) M}$.

⁵Throughout this paper, we do not include all details of the derivation if it involves simple calculations.

B. pdf of $f(g_k^e|g_k, \zeta_k; w_k)$

We first derive the joint pdf of $f(\mathbf{h}_k^e, \mathbf{h}_k, \mathbf{y}_k; w_k)$. From the Baye's theorem, we have

$$f(\mathbf{h}_k^e, \mathbf{h}_k, \mathbf{y}_k; w_k) = f(\mathbf{h}_k, \mathbf{y}_k|\mathbf{h}_k^e; w_k)f(\mathbf{h}_k^e),$$

where

$$f(\mathbf{h}_k, \mathbf{y}_k|\mathbf{h}_k^e; w_k) \sim \mathcal{CN}\left(\begin{bmatrix} \mathbf{0}_M & w_k \sqrt{c_k} \mathbf{h}_k^e \end{bmatrix}, \begin{bmatrix} \mathbf{I}_M & \sqrt{c_k} \mathbf{I}_M \\ \sqrt{c_k} \mathbf{I}_M & (1+c_k) \mathbf{I}_M \end{bmatrix}\right)$$

and $f(\mathbf{h}_k^e) \sim \mathcal{CN}(\mathbf{0}_M, \mathbf{I}_M)$.

Then, the conditional distribution of \mathbf{h}_k^e given \mathbf{h}_k and \mathbf{y}_k , $f(\mathbf{h}_k^e|\mathbf{h}_k, \mathbf{y}_k; w_k)$, becomes also the multivariate normal distribution that can be directly obtained from $f(\mathbf{h}_k^e, \mathbf{h}_k, \mathbf{y}_k; w_k)$ [54]. After some manipulations, we have $f(\mathbf{h}_k^e|\mathbf{h}_k, \mathbf{y}_k; w_k) \sim \mathcal{CN}(\boldsymbol{\mu}, \boldsymbol{\Sigma})$, where $\boldsymbol{\mu} = \frac{w_k \sqrt{c_k}}{1+w_k^2 c_k} (\mathbf{y}_k - \sqrt{c_k} \mathbf{h}_k)$ and $\boldsymbol{\Sigma} = \frac{1}{1+w_k^2 c_k} \mathbf{I}_M$. Then, since $g_k^e = \frac{(\mathbf{h}_k^e)^T \mathbf{a}_k}{\sqrt{M}}$, we can derive $f(g_k^e|\mathbf{h}_k, \mathbf{y}_k; w_k)$ from the transformation of the random vector as follows:

$$f(g_k^e|\mathbf{h}_k, \mathbf{y}_k; w_k) \sim \mathcal{CN}\left(\frac{w_k \sqrt{c_k}}{1+w_k^2 c_k} \left(\frac{\zeta_k}{\sqrt{M}} - \sqrt{c_k} g_k\right), \frac{1}{(1+w_k^2 c_k)M}\right).$$

Note that, by substituting (4) into (5), we have $\mathbf{a}_k = \frac{\mathbf{y}_k}{\zeta_k}$, which provides $f(g_k^e|\mathbf{h}_k, \mathbf{y}_k; w_k) = f(g_k^e|\mathbf{h}_k, \mathbf{a}_k, \mathbf{y}_k, \zeta_k; w_k) = f(g_k^e|\mathbf{h}_k, \mathbf{a}_k, g_k, \mathbf{y}_k, \zeta_k; w_k)$. Then, we finally have $f(g_k^e|\mathbf{h}_k, \mathbf{y}_k; w_k) = f(g_k^e|g_k, \zeta_k; w_k)$ since $f(g_k^e|\mathbf{h}_k, \mathbf{y}_k; w_k)$ is characterized by g_k and ζ_k .

APPENDIX E

The MMSE estimator for g_k is given by $\hat{g}_k = \mathbb{E}[g_k|\mathbf{r}_k, \mathbf{q}_k, \zeta_k; w_k] = \int g_k f(g_k|\mathbf{r}_k, \mathbf{q}_k, \zeta_k; w_k) dg_k$. Thus, the mean value of $f(g_k|\mathbf{r}_k, \mathbf{q}_k, \zeta_k; w_k)$, denoted by $\mu_{\hat{g}_k}$, is the MMSE estimator for g_k . The distribution of $f(g_k|\mathbf{r}_k, \mathbf{q}_k, \zeta_k; w_k)$ can be derived as follow:

$$\begin{aligned} f(g_k|\mathbf{r}_k, \mathbf{q}_k, \zeta_k; w_k) &= \frac{f(g_k, \mathbf{r}_k|\mathbf{q}_k, \zeta_k; w_k)}{f(\mathbf{r}_k|\mathbf{q}_k, \zeta_k; w_k)} \\ &= \frac{f(\mathbf{r}_k|g_k, \mathbf{q}_k; w_k) f(g_k|\zeta_k; w_k)}{\int f(\mathbf{r}_k|g_k, \mathbf{q}_k; w_k) f(g_k|\zeta_k; w_k) dg_k}. \end{aligned} \quad (39)$$

The pdf of $f(g_k|\zeta_k; w_k)$ in (39) is derived in Appendix D, while the pdf of $f(\mathbf{r}_k|g_k, \mathbf{q}_k; w_k)$ can be obtained from (7), which is given by $f(\mathbf{r}_k|g_k, \mathbf{q}_k; w_k) \sim \mathcal{CN}(g_k \mathbf{q}_k, \sigma_{n_k}^2 \mathbf{I}_{N_d})$. Then, after some manipulations, we finally have the pdf of $f(g_k|\mathbf{r}_k, \mathbf{q}_k, \zeta_k; w_k) \sim \mathcal{CN}(\mu_{\hat{g}_k}, \sigma_{\hat{g}_k}^2)$, where

$$\mu_{\hat{g}_k} = \frac{\mathbf{r}_k^\dagger \mathbf{q}_k + \sigma_{n_k}^2 \mu_{g_k} / \sigma_{g_k}^2}{\mathbf{q}_k^\dagger \mathbf{q}_k + \sigma_{n_k}^2 / \sigma_{g_k}^2} \text{ and } \sigma_{\hat{g}_k}^2 = \frac{\sigma_{n_k}^2 \sigma_{g_k}^2}{\mathbf{q}_k^\dagger \mathbf{q}_k \sigma_{g_k}^2 + \sigma_{n_k}^2}.$$

Thus, the MMSE estimator for g_k is given by $\hat{g}_k = \frac{\mathbf{r}_k^\dagger \mathbf{q}_k + \sigma_{n_k}^2 \mu_{g_k} / \sigma_{g_k}^2}{\mathbf{q}_k^\dagger \mathbf{q}_k + \sigma_{n_k}^2 / \sigma_{g_k}^2}$. In the same manner, we can derive the pdf

of $f(g_k^e|\mathbf{r}_k, \mathbf{q}_k, \zeta_k; w_k) \sim \mathcal{CN}(\mu_{\hat{g}_k^e}, \sigma_{\hat{g}_k^e}^2)$, where

$$\begin{aligned} \mu_{\hat{g}_k^e} &= \frac{w_k c_k}{1 + w_k^2 c_k} \left(\frac{\zeta_k}{\sqrt{c_k} M} - \frac{\mathbf{r}_k^\dagger \mathbf{q}_k + \sigma_{n_k}^2 \mu_{g_k} / \sigma_{g_k}^2}{\mathbf{q}_k^\dagger \mathbf{q}_k + \sigma_{n_k}^2 / \sigma_{g_k}^2} \right) \text{ and} \\ \sigma_{\hat{g}_k^e}^2 &= \frac{1}{(1 + w_k^2 c_k) M} + \left(\frac{w_k c_k}{1 + w_k^2 c_k} \right)^2 \frac{\sigma_{g_k}^2 \sigma_{n_k}^2}{\sigma_{g_k}^2 \mathbf{q}_k^\dagger \mathbf{q}_k + \sigma_{n_k}^2}. \end{aligned}$$

REFERENCES

- [1] A. D. Wyner, "The wire-tap channel," *AT&T Bell Labs. Tech. J.*, vol. 54, no. 8, pp. 1355–1387, Oct. 1975.
- [2] L. H. Ozarow and A. D. Wyner, "Wire-tap channel II," *AT&T Bell Labs. Tech. J.*, vol. 63, no. 10, pp. 2135–2157, Dec. 1984.
- [3] I. Csiszár and J. Körner, "Broadcast channels with confidential messages," *IEEE Trans. Inf. Theory*, vol. 24, no. 3, pp. 339–348, May 1978.
- [4] U. M. Maurer, "Secret key agreement by public discussion from common information," *IEEE Trans. Inf. Theory*, vol. 39, no. 3, pp. 733–742, May 1993.
- [5] R. Ahlswede and I. Csiszár, "Common randomness in information theory and cryptography—Part I: Secret sharing," *IEEE Trans. Inf. Theory*, vol. 39, no. 4, pp. 1121–1132, July 1993.
- [6] M. Bloch, A. Thangaraj, S. McLaughlin, and J. M. Merolla, "LDPC-based secret key agreement over the gaussian wiretap channel," in *Proc. IEEE ISIT*, July 2006, pp. 1179–1183.
- [7] M. Andersson, A. Khisti, and M. Skoglund, "Secret-key agreement over a non-coherent block-fading MIMO wiretap channel," in *Proc. IEEE ITW*, Sept. 2012, pp. 153–157.
- [8] O. Koyluoglu and H. El Gamal, "Polar coding for secure transmission and key agreement," in *Proc. IEEE PIMRC*, Sept. 2010, pp. 2698–2703.
- [9] C. W. Wong, T. Wong, and J. Shea, "Secret-sharing LDPC codes for the BPSK-constrained Gaussian wiretap channel," *IEEE Trans. Inf. Forensics Security*, vol. 6, no. 3, pp. 551–564, Sept. 2011.
- [10] W. T. Song, J. Choi, and J. Ha, "Perfect secrecy over binary erasure wiretap channel of type II," *IEEE Trans. Inf. Forensics Security*, vol. 7, no. 4, pp. 1414–1418, Aug. 2012.
- [11] A. Thangaraj, S. Dihidar, A. Calderbank, S. McLaughlin, and J.-M. Merolla, "Applications of LDPC codes to the wiretap channel," *IEEE Trans. Inf. Theory*, vol. 53, no. 8, pp. 2933–2945, Aug. 2007.
- [12] H. Mahdavi and A. Vardy, "Achieving the secrecy capacity of wiretap channels using polar codes," *IEEE Trans. Inf. Theory*, vol. 57, no. 10, pp. 6428–6443, Oct. 2011.
- [13] M. Andersson, V. Rathi, R. Thobaben, J. Kliewer, and M. Skoglund, "Nested polar codes for wiretap and relay channels," *IEEE Commun. Lett.*, vol. 14, no. 8, pp. 752–754, Aug. 2010.
- [14] G. Brassard and L. Salvail, "Secret-key reconciliation by public discussion," in *Advances in Cryptology — EUROCRYPT '93*, ser. Lecture Notes in Computer Science, T. Hellesteth, Ed. Springer Berlin Heidelberg, 1994, vol. 765, pp. 410–423.
- [15] C. Bennett, G. Brassard, C. Crepeau, and U. Maurer, "Generalized privacy amplification," *IEEE Trans. Inf. Theory*, vol. 41, no. 6, pp. 1915–1923, Nov. 1995.
- [16] C. H. Bennett and G. Brassard, "Quantum cryptography: Public key distribution and coin tossing," in *Proc. IEEE Int. Conf. Comput., Syst. and Signal Process.*, Bangalore, India, 1984, pp. 175–179.
- [17] A. K. Ekert, "Quantum cryptography based on bell's theorem," *Phys. Rev. Lett.*, vol. 67, pp. 661–663, Aug. 1991.
- [18] Y. Liu, S. Draper, and A. Sayeed, "Exploiting channel diversity in secret key generation from multipath fading randomness," *IEEE Trans. Inf. Forensics Security*, vol. 7, no. 5, pp. 1484–1497, Oct. 2012.
- [19] C. Ye, S. Mathur, A. Reznik, Y. Shah, W. Trappe, and N. B. Mandayam, "Information-theoretically secret key generation for fading wireless channels," *IEEE Trans. Inf. Forensics Security*, vol. 5, no. 2, pp. 240–254, June 2010.
- [20] K. Ren, H. Su, and Q. Wang, "Secret key generation exploiting channel characteristics in wireless communications," *IEEE Trans. Wireless Commun.*, vol. 18, no. 4, pp. 6–12, Aug. 2011.
- [21] T. L. Marzetta, "Blast training: Estimating channel characteristics for high capacity space-time wireless," in *Proc. 37th Annual Allerton Conf. on Commun., Control, and Comput.*, Monticello, U.S.A., Sept. 1999.
- [22] —, "Noncooperative cellular wireless with unlimited numbers of base station antennas," *IEEE Trans. Wireless Commun.*, vol. 9, no. 11, pp. 3590–3600, Nov. 2010.

- [23] J. Jose, A. Ashikhmin, T. L. Marzetta, and S. Vishwanath, "Pilot contamination and precoding in multi-cell TDD systems," *IEEE Trans. Wireless Commun.*, vol. 10, no. 8, pp. 2640–2651, Aug. 2011.
- [24] A. Khisti and G. W. Wornell, "Secure transmission with multiple antennas I: The MISOME wiretap channel," *IEEE Trans. Inf. Theory*, vol. 56, no. 7, pp. 2515–2534, July 2010.
- [25] J. Xiong, K.-K. Wong, D. Ma, and J. Wei, "A closed-form power allocation for minimizing secrecy outage probability for MISO wiretap channels via masked beamforming," *IEEE Commun. Lett.*, vol. 16, no. 9, pp. 1496–1499, Sept. 2012.
- [26] S. Im, H. Jeon, J. Choi, and J. Ha, "Secret key agreement under an active attack in MU-TDD systems with large antenna arrays," in *Proc. IEEE GLOBECOM*, Dec. 2013, pp. 1849–1855.
- [27] G. Geraci, M. Egan, J. Yuan, A. Razi, and I. B. Collings, "Secrecy sum-rates for multi-user MIMO regularized channel inversion precoding," *IEEE Trans. Commun.*, vol. 60, no. 11, pp. 3472–3482, Nov. 2012.
- [28] J. Zhu, R. Schober, and V. Bhargava, "Secure transmission in multi-cell massive MIMO systems," *IEEE Trans. Wireless Commun.*, vol. PP, no. 99, pp. 1–1, 2014.
- [29] C. Bennett, G. Brassard, C. Crepeau, and U. M. Maurer, "Generalized privacy amplification," *IEEE Trans. Inf. Theory*, vol. 41, no. 6, pp. 1915–1923, Nov. 1995.
- [30] M. Guillaud, D. T. M. Slock, and R. Knopp, "A practical method for wireless channel reciprocity exploitation through relative calibration," in *Proc. IEEE ISSPA*, Aug. 2005.
- [31] T.-H. Chou, V. Tan, and S. Draper, "The sender-excited secret key agreement model: Capacity, reliability and secrecy exponents," *IEEE Trans. Inf. Theory*, vol. PP, no. 99, pp. 1–1, 2014.
- [32] N. Wang, N. Zhang, and T. Gulliver, "Cooperative key agreement for wireless networking: Key rates and practical protocol design," *IEEE Trans. Inf. Forensics Security*, vol. 9, no. 2, pp. 272–284, Feb. 2014.
- [33] X. Zhou, B. Maham, and A. Hjørungnes, "Pilot contamination for active eavesdropping," *IEEE Trans. Wireless Commun.*, vol. 11, no. 3, pp. 903–907, Mar. 2012.
- [34] D. Kapetanovic, G. Zheng, K.-K. Wong, and B. Ottersten, "Detection of pilot contamination attack using random training and massive MIMO," in *Personal Indoor and Mobile Radio Communications (PIMRC), 2013 IEEE 24th International Symposium on*, Sept. 2013, pp. 13–18.
- [35] S. Im, H. Jeon, J. Choi, and J. Ha, "Robustness of secret key agreement protocol with massive MIMO under pilot contamination attack," in *Proc. IEEE ICTC*, Oct. 2013, pp. 1053–1058.
- [36] J. Xiong, K.-K. Wong, D. Ma, and J. Wei, "A closed-form power allocation for minimizing secrecy outage probability for MISO wiretap channels via masked beamforming," *IEEE Commun. Lett.*, vol. 16, no. 9, pp. 1496–1499, Sept. 2012.
- [37] N. Romero-Zurita, M. Ghogho, and D. McLernon, "Outage probability based power distribution between data and artificial noise for physical layer security," *IEEE Trans. Signal Process. Lett.*, vol. 19, no. 2, pp. 71–74, Feb. 2012.
- [38] P. Pinto, J. Barros, and M. Win, "Secure communication in stochastic wireless network part I: Connectivity," *IEEE Trans. Inf. Forensics Security*, vol. 7, no. 1, pp. 125–138, Feb. 2012.
- [39] C. H. Bennett and G. Brassard, "Quantum cryptography: Public key distribution and coin tossing," in *Proc. IEEE Int'l Conf. Computers, Systems and Signal Process.*, Dec. 1984, pp. 175–179.
- [40] C. H. Bennet, "Quantum cryptography using any two nonorthogonal states," *Phys. Rev. Lett.*, vol. 68, no. 21, pp. 3121–3124, May 1992.
- [41] A. K. Ekert, "Quantum cryptography based on Bell's theorem," *Phys. Rev. Lett.*, vol. 67, no. 6, pp. 661–663, Aug. 1991.
- [42] W. K. Wootters and W. H. Zurek, "A single quantum cannot be cloned," *Nature*, vol. 299, no. 5886, pp. 802–803, Oct. 1982.
- [43] H. V. Poor, *An Introduction to Signal Detection and Estimation*, 2nd ed. NY: Springer-Verlag, 1994.
- [44] J. Choi, *Optimal Signal Combining and Detection: Statistical Signal Processing for Communications*. Cambridge University Press, 2010.
- [45] D. Slepian and J. K. Wolf, "Noiseless coding of correlated information sources," *IEEE Trans. Inf. Theory*, vol. IT-19, no. 4, pp. 471–480, July 1973.
- [46] J. L. Carter and M. N. Wegman, "Universal classes of hash functions," *J. Comp. Syst. Sci.*, vol. 18, no. 2, pp. 143–154, Apr. 1979.
- [47] A. W. Eckford and W. Yu, "Rateless Slepian-Wolf codes," in *Proc. 39th Asilomar Conf. Signal, Syst., Comput.*, Pacific Grove, CA, Oct. 2005, pp. 1757–1761.
- [48] J. Jiang, D. He, and A. Jagmohan, "Rateless Slepian-Wolf coding based on rate adaptive low-density-parity-check codes," in *Information Theory, 2007. ISIT 2007. IEEE International Symposium on*, June 2007, pp. 1316–1320.
- [49] K. Gomadam, H. Papadopoulos, and C.-E. Sundberg, "Techniques for multi-user MIMO with two-way training," in *Proc. IEEE ICC*, May 2008, pp. 3360–3366.
- [50] J. Jose, A. Ashikhmin, P. Whiting, and S. Vishwanath, "Channel estimation and linear precoding in multiuser multiple-antenna TDD systems," *Vehicular Technology, IEEE Transactions on*, vol. 60, no. 5, pp. 2102–2116, Jun 2011.
- [51] M. K. Simon and M.-S. Alouini, "Exponential-type bounds on the generalized Marcum Q-function with application to error probability analysis over fading channels," *IEEE Trans. Commun.*, vol. 48, no. 3, pp. 359–366, Mar. 2000.
- [52] G. Corazza and G. Ferrari, "New bounds for the Marcum Q-function," *IEEE Trans. Inf. Theory*, vol. 48, no. 11, pp. 3003–3008, Nov. 2002.
- [53] M. Bloch, J. Barros, M. R. D. Rodrigues, and S. W. McLaughlin, "Wireless information-theoretic security," *IEEE Trans. Inf. Theory*, vol. 54, no. 6, pp. 2515–2534, June 2008.
- [54] M. L. Eaton, *Multivariate Statistics: a Vector Space Approach*. New York: John Wiley and Sons, 1983.